12-2006

OPTIMIZING PRODUCTION METHODS FOR ARTIFICAL SILK PROTEINS THROUGH BIOREACTOR AND PURIFICATION STUDIES OF RECOMBINANT PROTEINS EXPRESSED FROM Pichia pastoris

Aaron Ramey
Clemson University, rameya@clemson.edu

OPTIMIZING PRODUCTION METHODS FOR ARTIFICAL SILK PROTEINS THROUGH BIOREACTOR AND PURIFICATION STUDIES OF RECOMBINANT PROTEINS EXPRESSED FROM *Pichia pastoris*

A Thesis
Presented to
the Graduate School of
Clemson University

In Partial Fulfillment
of the Requirements for the Degree
Master of Science
Polymer and Fiber Science

---

by
Aaron Thomson Ramey
December 2006

Accepted by:
Dr. Michael Ellison, Committee Chair
Dr. Sarah Harcum
Dr. Gary Lickfield

ABSTRACT

Advancements in the field of biomaterials are soon to make the production of a recombinant silk fiber a reality. A gene was constructed which utilized components from both the dragline silk of *Nephila clavipes* and nematode collagen. For this engineered protein, the yeast strain *Pichia pastoris* was chosen to be the host organism due to its ease of genetic manipulation and its ability to secrete proteins in soluble forms. Previous research has shown *P. pastoris* to have comparatively low amounts of specific protein productivity. Therefore, in order to produce adequate amounts of recombinant protein, this problem must be compensated for by obtaining extremely high cell densities (Charoenrat, 2005). The main focus of this study is to optimize the fermentation parameters of transgenic yeast cultures within a bioreactor in order to increase the yield of the recombinant protein. Through media improvement and feed pump control, cell densities of 350 optical density (OD) were obtained. In conjunction with optimization experiments, concentration and purification methods revealed insight into this material's potential for future processing. Additionally, comparative studies with natural spider silk revealed temperature fluctuations within the spinneret region that may be an integral component in learning how to assemble our recombinant proteins.

DEDICATION

This thesis is dedicated to my best friend, Jeff Willey. His passion for science and determination towards constant self-improvement was a source of inspiration and motivation. He was always there to offer a helping hand and never asked for anything in return. I will forever be grateful for all of his love and support. I wish there were more words to express my gratitude, but these are all have. Thank you.

ACKNOWLEDGMENTS

I would like to thank my advisor Dr. Michael Ellison for his support, guidance, and for giving me this opportunity.

Also, thanks to my committee members Dr. Sarah Harcum and Dr. Gary Lickfield for lending their expertise to this project. Thanks to Dr. Albert Abbott who was an integral part of this project as well.

I would like to thank The School of Materials Science and Engineering for making this degree possible. Thanks to all of the faculty and staff members for their friendship and support over these past two years.

I would like to also acknowledge David White with the School of MS&E for the assistance and technical support he supplied with the spiders. Thanks also to Mary Caldwell with the Department of Bioengineering and Dr. Peifeng Chen at Invitrogen Corporation for their friendship and invaluable help in the laboratory.

I am extremely grateful for my parents, Albert and Mary Jane Ramey. This degree would not have been possible it were not for their constant love and support. Also, thanks to Ashley and Leigh, two of the best sisters and friends anyone could ask for. Finally, I would like to acknowledge all of the friends I have made along the way that have helped to shape my Clemson experience.

TABLE OF CONTENTS

Table of Contents (Continued)

LIST OF FIGURES

List of Figures (Continued)

LIST OF TABLES

INTRODUCTION

Through cloning technology, the Biologically-inspired Advanced Materials (BAM) Research Group is synthetically creating silk proteins in order to manufacture biologically-inspired fibers with unmatched performance capabilities. Scientists from Clemson University's School of Materials Science and Engineering, Departments of Genetics and Biochemistry, Bioengineering, and Physics have been collaborating and utilizing their specific areas of expertise on this project for more than ten years. It is the hope and ultimate goal of this project to develop fibers that benefit from both nature's desirable physical properties and its ability to produce biodegradable, sustainable materials.

Biomimetics (also known as bionics or biomimicry), first termed at a cybernetics conference in 1960, is the science that investigates methods and systems found in nature to design engineered systems and technology to mimic these natural systems (Bar-Cohen, May 13, 2003). The benefits of modeling technology after nature are immense because evolutionary pressure has forced biological systems to become highly optimized and efficient (Passino, 2005). The field itself has a long history, even though the exact origins can not be traced. For example, its practice can be seen as far back as Leonardo de Vinci's sketches of flying machines and boats (Azuma, 2006). Until recently, Swiss engineer George de Mestral was the only pioneer in the field to experience great commercial success. Mestral developed Velcro by imitating the 'hook and latch' method he observed when burrs attached to his dog's fur (Forbes, 2005). Today, the advent of new technologies has been a gateway towards allowing humanity's natural inspirations to become realities.

The influence of biomimetics can be seen in virtually all disciplines such as biology, computer engineering, and even politics. When discussing biology, there are typically three areas that serve as models for developing technologies. Biological mechanisms such as the 'hook and latch' model can be imitated. Also, organizational principles can be developed from studying the social patterns of animal groups, such as migratory birds. The third area, with which this project is concerned, deals with mimicking modes of producing chemical compounds in order to develop novel ones (Benyus, 1998). The manufacturing of artificial polymers using this method is greatly desired today because of the growing concerns for energy needs and reusable materials.

In general, polymers are long chain molecules consisting of repeating structural units joined by covalent bonds. The use of polymers is wide-spread and can be found in applications ranging from engineering plastics to synthetic fibers. Unfortunately, conventional production of polymers has been plagued with obstacles such as high energy costs, non-biodegradable materials, and harmful waste products. For example, Kevlar fibers are produced under elevated temperatures and pressures and are spun from highly concentrated sulfuric acid solutions (Viney, 1992). Advances in genetics and molecular engineering have allowed scientists to look at overcoming these problems by modeling nature's method for polymer synthesis.

Polypeptides, or proteins, are polymeric macromolecules synthesized by biological organisms. They are essential components for life that participate in every process in a cell. Proteins are composed of amino acids, which are encoded by the organism's genome. These amino acids are joined together by peptide linkages, and depending upon their order, self-assemble into biologically-active conformations. Just as polymers are composed of monomeric units, proteins benefit from the combination of different amino acids whose

chemical constituents and specific placement determine unique physical properties such as strength, flexibility, and solubility. Cloning technologies have enabled scientists to tailor these properties by constructing the protein on the molecular level and then introducing the genetic sequence into other biological systems that can read and express these codes into proteins.

These genetically engineered proteins, more commonly known as either recombinant or heterologous proteins, were first described by Stanley N. Cohen in 1973 in a paper that outlined a method for isolating and inserting genes into other biological systems (Cohen, 1973). In 1977, *Escherichia coli* became the first bacterium host to produce a commercially biologically active protein, human somatostatin, from a eukaryotic source (Itakura et al., 1977). Since that time, the area of recombinant DNA has seen enormous growth, resulting in the production of many recombinant proteins of industrial and medical significance. The emergence of bioreactors that are able to yield high cell densities has also served as a major breakthrough, enabling the ease of production. Examples of some of the well-known proteins synthesized through recombinant technology include insulin, erythropoietin, tissue plasminogen activator, factor VII for treatment of hemophilia, human α-interferon, hepatitis B surface antigens, and enzymes such as calf prochymosin and *Aspergillus* glucoamylase (Gellissen et al., 1992).

Two of the most prevalent expression systems available for recombinant protein production are *E. coli* and *P. pastoris*. Since its introduction as a marketable vector in 1977, *E. coli* has become the benchmark for molecular cloning for a number of well-documented reasons. Probably the most important advantage for using *E. coli* is its ease of genetic manipulation (Lee and Lee, 2003). It is fairly easy to manipulate due in part to its relatively small genome and long history of study in laboratories (Blattner et al., 1997). Furthermore,

its prevalence in laboratories has facilitated the development of commercially available genome-wide microarrays containing all of the open reading frames and intergenic regions (Selinger et al., 2000).

The major drawback in using *E. coli* as a recombinant protein expression system is its inconsistent behavior with respect to soluble expression of eukaryotic proteins (Daly and Hearn, 2005). Eukaryotic proteins expressed in *E. coli* often aggregate and form insoluble material, termed inclusion bodies. Inclusion bodies require additional purification steps in order to yield a biologically-active product (Marston, 1986). Additionally, proteins which need post-translational modifications such as glycosylation, proline isomerization, lipidation, sulphation, disulfide isomerization, and phosphorylation can not be completely produced in *E. coli*, as it lacks the machinery to perform these chemical modifications (Lueking et al., 2000). Another problem for recombinant proteins expressed in *E. coli* is the non-cleaved amino-terminal methionine. This methionine can change the stability of the protein in a patient receiving the recombinant protein as a drug; however, this residue can be removed chemically (Chaudhuri, 1999).

Proteins that have been difficult to express in *E. coli* because of post-translational modification issues have subsequently been introduced into the methylotrophic yeast strain *P. pastoris* for production (Monsalve et al., 1999). The products from this system tend to be both soluble and appropriately folded, although some post-translational modifications are not identical to the original species. Results from a comparative study preformed by Lueking et al. highlight *P. pastoris*'s ability to out-perform *E. coli* when expressing eukaryotic proteins. Out of the 29 proteins that were cloned into each of the two hosts, all were found to be soluble in *P. pastoris*, compared to the nine soluble proteins in *E. coli* (Lueking et al., 2000). *P. pastoris* is also easy to genetically manipulate (Cregg et al., 1993); however, it has

fewer cloning vectors and selection methods. Also, *P. pastoris's* aerobic growth allows for high cell yields, which in turn allows for high intracellular and extracellular recombinant protein production with limited byproduct formation, such as ethanol and acetic acid (Daly and Hearn, 2005). In comparison to the yeast *Saccharomyces cerevisia*, *P. pastoris* has been shown to produce ten times the biomass in fermentations.

P. pastoris is one of the few species of yeast that is able to metabolize methanol as its sole carbon source. Other strains able to utilize this form of carbon and energy are *Candida*, *Torulopsis*, and *Hansenula* (Lee, 1980). Along with *H. polymorpha*, *P. pastoris* has been thoroughly studied and documented as a model organism for recombinant protein production (Gleeson, 1988). Both of these systems employ a fusion between the foreign gene sequences and a strong methanol promoter which allows for the metabolism of methanol (Gellissen et al., 1992). Because of this coupling, the presence of methanol will cause transcription and translation of not only the gene encoding for the enzyme, but also for the recombinant protein (Tschopp et al., 1987). This promoter, known as the alcohol oxidase 1 gene (AOX1), is known to be a tightly regulated promoter for recombinant protein expression (Cregg et al., 1993). Normally, the yeast cells are initially grown on either glycerol or glucose, causing repression of the AOX1 promoter, in order to reach high cell densities. Once the desired cell density is reached, methanol is supplied as the sole carbon source, which also induces expression of the desired protein. Yeast cells grow slowly on methanol, thus alternate carbon sources such as glycerol are typically used to obtain cell densities large enough to justify induction (Inan and Meagher, 2001). Glucose is not commonly used because studies have shown it is more difficult to reverse repression of the promoter by methanol, and less biomass is obtained (Faber, 1995) (Sola et al., 2004).

P. pastoris contains two copies of the AOX gene (AOX1 and AOX2); however, the AOX1 gene is responsible for 85% of the alcohol oxidase regulation within the cell and is therefore the promoter used in recombinant protein expression (Inan and Meagher, 2001). The AOX1 promoter expression cassette is inserted into the *P. pastoris* genome, and depending upon its placement, yields various phenotypes of the strain (Breirley, 1990). *P. pastoris* has three different phenotypes which are able to utilize methanol, Mut^+, Mut^S, and Mut^-. Mut^+ strains contain a functional copy of the AOX1 gene, resulting in a phenotype indistinguishable from the wild-type methanol utilizing strain (Inan and Meagher, 2001). Placing the recombinant protein expression cassette within the AOX1 gene causes a Mut^S phenotype, which has slow growth on methanol (Romanos et al., 1992). A Mut^- strain results when the expression cassette disrupts both the AOX1 and AOX2 genes, giving a strain which is unable to metabolize methanol as its sole carbon source (Chiruvolu, 1997). The GS115 *P. pastoris* yeast strain is an example of one that has the Mut^+ strain, which is the strain exclusively used in the studies relative to this research project. The GS115 strain also includes a mutation in the histidine dehydrogenase gene (HIS4), which is used to identify successful transformants (Inan and Meagher, 2001).

Table A Examples of Recombinant Proteins Expressed in *P. pastoris* Under the Control of the AOX1 Promoter

Protein	Reference
HBsAg (S)	Cregg et al. 1987
Human EGF	Siegel et al. 1989
Bovine Lysozyme	Digan et al. 1989
Streptokinase	Hagenson et al. 1989
Human TNF	Sreekrishna et al. 1989
Aprotinin	Vedvick et al. 1991
Tetanus C	Clare et al. 1991
HAS	Provow cited in Buckholz & Gleeson 1991
Human IGF1	Breierley cited in Buckholz & Gleeson 1991
Il-2	Velicelebi cited in Buckholz & Gleeson 1991
HIV gp120	Romanos cited in Buckholz & Gleeson 1991

adopted from (Charoenrat, 2005)

The availability of methylotrophic yeast strains that are able to produce the recombinant proteins described above has enabled researchers in many fields to explore the use of recombinant technology. One such area which has benefited from cloning techniques is textiles. Even though recombinant silk production is a recent endeavor, the properties of spider silk have been known and exploited for centuries. Various cultures have been reaping the benefits from this remarkable fiber in various ways. Tribes in New Guinea have used spider webs for hats designed as raingear. Multiple fishing societies incorporate spider silk into nets. Even Americans in World War I used spider silk strands as the cross bars for targets in telescopic gun-sites. Research into spider silk's desirable properties have prompted numerous articles over the past 150 years (Lewis et al., 1996). However, significant progress into the understanding of silk's unique material properties only started to become known about 30 years ago, with the research of Work, Gosline, and Tillinghast. Since then, the emergence of biomaterials has brought about a revival in silk studies, leading the way to the next generation of spider researchers exemplified by Kaplan, Vollrath, and Hayashi.

Silk is not unique to spiders, even though they are the most widely known producers (Viney, 1992). Silk worms such as *B. mori* have a 4,000 year old history in garment making. (Hyde, 1984). Additionally, various insects produce silk protein to aid in locomotion, egg sac and habitat construction, and prey capture (Lucas, 1964). However, spiders have been the main focus of silk study in the very recent past. They are unique from insects in that they depend on silk throughout their life cycle (Vollrath, 1992). *N. clavipes* and *Araneus diadematus* are two of the most highly studied and highly evolved producers of silk. These orb-weaving spiders have been desired for different reasons. *A. Diadematus* is a very small and common garden spider. *N. clavipes* is large in size, easy to dissect, and produces large quantities of silk (Viney, 1992). In terms of material properties, *N. clavipes'* silk is preferable. In general, silk

has a unique combination between strength (stress applied at break), stiffness (modulus at yield point), toughness (energy required to break), and elasticity (ability to return to original conformation after an applied strain is removed). The material properties of silk produced by *N. clavipes* makes it preferred over other types of silk: it is nearly as strong and has a much greater toughness than high-performance polyamide fibers such as Kevlar (Gosline et al. 1986, Kaplan et al. 1991). Figure A shows a stress/strain curve in which common material science terminology is defined to understand the tensile properties of spider silk.

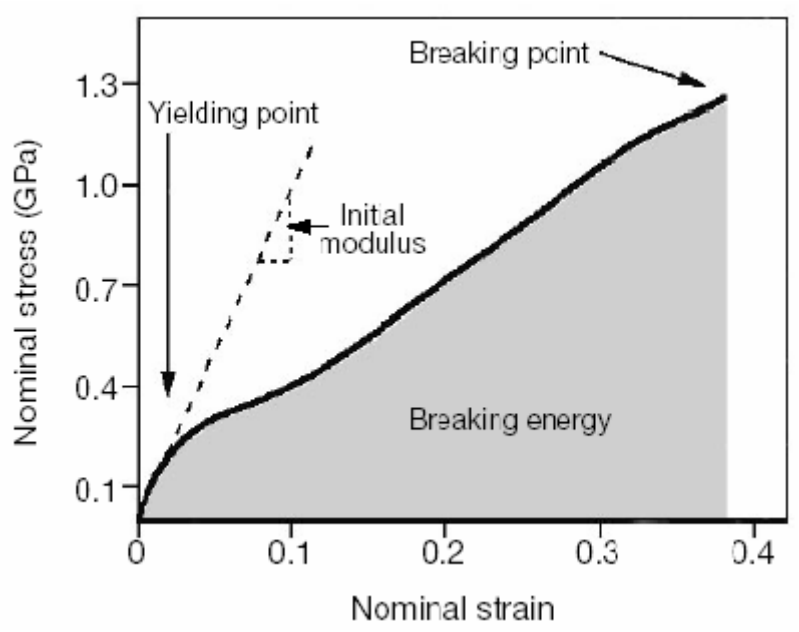

Figure A Schematic of the Definitions: Strength, Stiffness, Toughness, Elasticity, Stress, and Strain (Vollrath and Knight, 2001)

The first fibrous protein comprising *N. clavipes* dragline silk from the major ampullate gland, known as spidroin 1 or MaSp1, was isolated from cDNA clones and published in 1990 (Xu, 1990). The amino acid structure predicted from that research, however, did not account for the complete amino acid sequence of dragline silk. Thus, more research was conducted and the second protein, spidroin 2 or MaSp2, was sequenced and published in 1992 (Hinman, 1992). The cloning of spidroin-like proteins into *P. pastoris* is the basis for

this thesis, and therefore previous work done by the BAM group at Clemson University will be summarized to serve as background information for the subsequent chapters.

The dissertation work of Florence Teulé in 2003 outlines the methods for engineering spidroin-like proteins in *P. pastoris* for the production of intracellular and secretory recombinant proteins. In her research, she explored the effects that the basic structural components (amino acids) had on the resulting stability and solubility of the protein. Natural spider dragline silk is composed of two hydrophobic amino acid repeat sequences consisting of alanine and alanine-glycine regions. Both of these sequences have been predicted to assume conformations resulting in the crystalline portion of the silk. In theory, each chain can interlock with an adjacent chain via hydrophobic interactions. The glycine side of the polypeptide chain would have less hydrophobic interactions than the alanine portion. With more interactions, alanine sequences as apposed to alanine-glycine sequences would have a greater binding energy. Therefore, more alanine regions would theoretically create β-sheet structures with a higher degree of orientation (Hayashi, 1999). Further evidence supporting this theory can be seen in minor ampullate silk, which has a lower tensile strength corresponding to a lower proportion of alanine repeat sequences. Hayashi also mentions that anti-parallel β-sheet structures have been observed to be poorly hydrated. Thus, the hypothesis becomes that crystals aligned parallel to the fiber axis contain higher amounts of alanine repeats, thereby leading to a greater tensile strength for the resulting fiber (Teulé, 2003).

Testing the importance of these alanine-rich motifs, Teulé genetically engineered three spidrion-1 like proteins containing varying amounts of alanine (normal alanine content, low alanine content, and no alanine). In addition, she also engineered three copolymers of these sequences combined with collagen, mimicking the silk-collagen structures found in the

byssus thread of marine mussels. Each of the six engineered plasmids containing both the gene constructs and the expression vector pPICZαA (Figure B) from Invitrogen were transformed into the *P. pastoris* host strain GS115 from Invitrogen's EasySelect™ *Pichia* Expression Kit (version C). The three spidroin-1-like constructs with normal, low, and no alanine were given the respective names pαASpi 1-ALA, pαASpi 1-LA, and pαASpi 1-NA (abbreviated ALA, LA, and NA). Copolymers of the collagen and silk constructs were named pαACoSpi 1-ALA, pαACoSpi 1-LA, and pαACoSpi 1-NA (abbreviated COALA, COLA, and CONA).

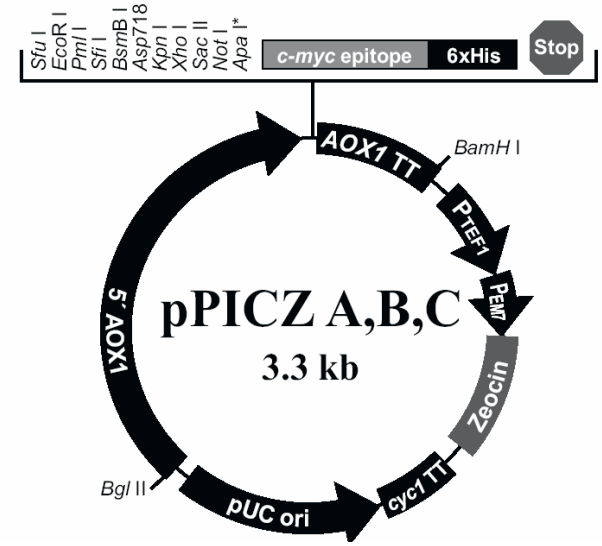

Figure B Schematic of pPICZαA Vector Depicting AOX1 Promoter Necessary for Expression: the zeocin marker is used for selection for antibody-resistant strains, the *c-myc* epitope is used for detection of protein with anti-*myc* antibody (Evans et al 1985), and the 6X histidine repeat sequence is used for detection of protein with anti-his antibody (Lindner et al 1997) (Invitrogen's *Pichia Expression Vectors for selection on Zeocin and Purification of Recombinant Proteins* product manual; catalogue number V190-20, 2001).

Results from both protein staining and Western Blotting techniques concluded successful expression of both spidroin and collagen-spidroin from yeast (Teulè, 2003). Overall, the copolymer constructs had higher expression of soluble recombinant protein over the homopolymer constructs. Even though collagen is known to be insoluble, it was

hypothesized by Teulé that the juxtaposition of the spidroin and collagen sequences allowed for easier dissociation in solvent. Out of the three copolymer constructs, CONA (as well as NA) produced significantly less recombinant protein than the constructs containing normal and low alanine amounts. Since these strains lacked the characteristic polyalanine motifs, it was conjectured that the alanine content encouraged the intracellular stability of the protein. Both COALA and COLA strains consistently secreted the collagen-spidroin proteins in stable dimers, both being at molecular weights of around 63 kDa. Also, the majority of the protein in both strains was expressed intracellularly as opposed to being secreted outside of the cell.

This thesis explores three main areas related to the recombinant silk protein production. The first chapter deals with optimizing the bioreactor conditions for producing this protein. The second chapter investigates purification methods for the protein being produced by fermentation. Finally, the third chapter describes comparative studies conducted on natural spider silk, which were undertaken to help develop processes for recombinant protein spinning in the future.

CHAPTER ONE

Fermentation of the Yeast Strain Pichia pastoris for the Production of Recombinant Silk/Collagen Protein

BACKGROUND

Yeast live and propagate in various natural habitats, often in cohabitation with other microorganisms including fungi, bacteria, and protozoa as well as more advanced forms of life, such as plants, insects, and warm-blooded animals. The majority of yeast have a saprophytic life, meaning they grow on inert, organic substrates. However, parasitic forms that rely on a host to provide the necessary nutrients are also known. Yeast sometimes compete for nutrients with other microorganisms that are cohabitating on a substrate. Also, some natural substrates produce antibiotics that inhibit the growth of yeast, affecting their populations. As a result, some strains of yeast have a remarkable variation in sensitivity to various antibiotics that can be utilized in controlled laboratory settings. In addition, yeast can also be sensitive to some of the metabolic products from bacteria that can inhibit growth, such as acetic acid. Another common occurrence is the consumption of yeast by protozoa, insects, and other animals. Even though these organisms are consuming yeast as a food source, they facilitate the distribution of yeast by incasing the yeast within body cavities or allowing them to adhere exteriorly (Phaff, 1978).

Yeast, like other unicellular organisms, are able to withstand environmental fluctuations through internal adaptations. This collection of complex cellular responses has stemmed from millions of years of selective evolution, which has exposed this organism to extreme atmospheric conditions. These external challenges can disturb the homeostatic

conditions of the cell, thereby interrupting metabolic processes necessary for propagation. To counteract this issue and reduce stress, yeast can re-program genomic expression according to the cell's requirements for adequate growth. This response enables yeast to respond to environmental stimuli at essentially every level of cellular organization (Gasch, 2002).

Yeast, probably the oldest known domesticated organism, was first used in Sumeria and Babylonia in 6000 B.C. for the purpose of brewing beer (Feldman, 2005). Various strains of this species also date back to Egypt where they were used in grape cultivation and dough leavening. The English word *yeast*, the German word *hefe,* and the Dutch word *guist* are derived from the west-germanic phrase *haf-jon* meaning 'the potential to leaven,' referring to the yeast's ability to anaerobically release carbon dioxide. Even the word *enzyme*, meaning 'in yeast' has been termed as a means to describe the organic compounds yeast use to ferment sugar. These desired properties of yeast have carried them through thousands of years of research, uncovering their great potential in the food and medical industries of today. Table 1.1 below highlights the momentous events associated with yeast through history.

Table 1.1 History of Yeast as a Domesticated Organism

Approximate Date	Event
6000 B.C.	Beer brewing
1680	First microscopic image (van Leeuwenhoek)
1835	Alcohol fermentation
1839	Sugar used as yeast food source
1857	Correlation between fermentation and metabolism (Pasteur)
1876	'Etudes sur la levure de bière' (Pasteur)
1877	Term *enzyme* first used (Kŭhne)
1880	Single cells and strains used in brewing (Hansen)
1883	Alcohol and CO2 from cell-free extracts (Buchner)
1915	Production of glycerol
1920	Yeast physiology
1949	First genetic map (Lindegren); mating type system
1930	Taxonomy (Kluyver)
1966	First tRNA structures
1978	First transformation (Hinnen, Hicks, and Fink)
1990	First commercial pharmaceutical product from recombinant yeast (Hepatitis B vaccine)
1996	Completion of yeast genome project

adopted from (Feldman, 2005)

Yeast comprising approximately 700 different species were introduced as an experimental organism in the mid 1930's. Since that time, yeast biotechnology has expanded into various fields such as fermentation, food, chemical, and health-care industries, biological and biomedical research, and environmental technologies (Feldman, 2005). These fields have further expanded with the introductionn of bioreactors, which have transformed yeast culturing into a highly-controlled operation. As opposed to shake flasks, bioreactors regulate the environment such that cells can grow under optimal conditions for a longer period of time. Conditions such as temperature, pH, and nutrient and oxygen requirements can be monitored and controlled. In fact, protein production in *P. pastoris* has been shown to increase 140% when scaled-up from a shaker to a bioreactor (Cino, 1999).

Bioreactors can be operated in fed-batch mode, where fresh media is added to the culture, preventing nutrient limitations. In some instances, the nutrients are gradually fed

into the bioreactor in order to avoid both substrate limitation and inhibition (Charoenrat, 2005). Shake flasks are only easily operated in batch mode because of size limitations, thus cells are cultured only in the nutrients present at the time of inoculation. Both shake flasks and bioreactors can be mixed to increase oxygen transport; however, in shake flasks oxygen becomes limited as the cell density increases, which can result in anaerobic metabolism with associated ethanol and acetate secretion. The oxygen transfer rate in shake flasks is proportional to the agitation rate, but as cell densities increase, the cells consume oxygen faster than it can be supplied. In bioreactors, oxygen levels can be monitored and controlled. Specifically, dissolved oxygen levels can be controlled with the use of aeration, agitation, and external oxygen (Ohashi, 1999). Bioreactors can also control the pH levels though the addition of acid and base solutions. Shake flasks are not equipped with pH meters; therefore the acid production from growing cells can cause pH levels to reach lethal limits. Furthermore, the tightly-regulated bioreactor allows for better control necessary when using a methanol feed for induction phases in *P. pastoris*. Methanol utilization as the carbon source has higher than normal oxygen requirements compared to glucose and glycerol. In order to achieve high levels of recombinant protein productivity, the methanol levels must be balanced to provide enough carbon to maintain cell viability and recombinant protein expression and to prevent methanol cytotoxic levels (Mayson, 2003). Bioreactors can often be equipped with software that monitors and stores culture conditions, which allows for graphical representation of the environment within the fermentation vessel. Additionally, the system's records can be used for troubleshooting.

This chapter investigates the growth of yeast cells on various media and feed protocols. Also, the production of the recombinant silk protein was examined.

MATERIALS AND METHODS

Product Description

The bioreactor used in this study was Sartorius BBI Systems GmbH's bench-top scale fermenter type BIOSTAT®B. This model is designed for the cultivation of either microorganisms or tissue cell cultures in either continuous, batch, or fed-batch modes. For the purpose of this thesis, the fed-batch mode fermentations of the *P. pastoris* yeast strain GS115 containing the recombinant spider silk/collagen copolymer were conducted.

The glass culture vessel has a working volume of 5 liters. In association with this vessel, a control unit monitored and controlled the various environmental conditions within the vessel. A thermometer inserted into the culture vessel was attached to the control unit containing an internal thermostat. This thermostat controlled both the heating and cooling functions in conjunction with a glass water jacket surrounding the vessel. An external water cooling unit was kept at a constant 15°C. An oxygen-sensing electrode inserted into the vessel monitored the amount of dissolved oxygen within the culture. The oxygen transfer rate was controlled by both agitation and oxygen supplementation to maintain a dissolved oxygen setpoint. Three, six-bladed metal disc impellers were used in the vessel to stir the liquid. Once the maximum agitation speed was reached (1200 rpm), oxygen from a tank was mixed with air to sparge the vessel. The pH was monitored using a pH electrode inserted into the vessel. Depending upon whether the pH needed to be raised or lowered, the readings from the pH probe signaled either an influx of acid (HCl, 2N solution) or base (NH_4OH, 25% volume/volume). Acid and base solutions were fed from glass bottles through 14 gauge tubing, using pump rates managed by the control unit.

Sartorius BBI's MFCS/win 2.1 was the software used to record the data from the fermentations. This program is a batch oriented Supervisory Control and Data Acquisition

(SCADA) System used specifically for fermentation processes. The software was not only able to record the data but it also displayed the information in a graphical representation for easy monitoring of the environmental conditions within the vessel. Also, it featured an extensive reporting system with export filters for alternate software programs that enabled efficient monitoring of the growth rates in Microsoft Excel.

Figure 1.1 Picture of BIOSTAT® BPlus from Sartorius AG, Similar to the Bioreactor Used for this Study.

Log Phase Experiment

Prior to the bioreactor studies, the growth characteristics of the yeast were determined in order to identify the exponential growth phase. Yeast cells were obtained from a stock culture stored at -80°C. Once thawed, a sterile loop was inserted into the cryovial tube and the cells were streaked for isolation onto a culture plate containing sterile YPDS media (Appendix 1.A) + 1X 100 μg/ml Zeocin (cells containing the recombinant protein were Zeocin resistant). The plates were then incubated at 36°C for 2 days. For the exponential phase identification, a single colony was selected from the plate and used to inoculate a 250 ml sterile shake flask containing 50 ml of sterile buffered minimal glycerol histidine (BMGH) media (Invitrogen) (Appendix 1.B). The cells were cultured at 30°C and agitated at 300 rpm using a bench-top incubator shaker for a period of 30 hours. Cell

densities were determined by optical density (OD) measurements of the culture, obtained periodically by measuring a 1 ml sample in a Spectronic® 20 Genesys™ spectrometer at wavelength 600 nm. This instrument measured the amount of light absorbed by a solution, where the OD of a culture was proportional to the cell density or biomass. Samples were diluted with water, if necessary, such that the absorbance reading was below 0.5 units. Frozen stock colonies were made from the plates by isolating the remaining cells and storing them in a sterile 15% glycerol solution in cryovial tubes at -80°C.

Preparation of Bioreactor

Batch media components (Appendix 1.C) were added to the fermentation vessel first. The batch media totaled 1 liter at the start of fermentation. The calcium, magnesium, and trace metal components (Appendix 1.D) were added after the vessel was autoclaved because of their tendency to precipitate at high temperatures. The biotin and histidine components were added later as well because these components degrade at high temperatures. The magnesium and calcium solutions were autoclaved separately, while the trace metal, biotin, and histidine solutions were filter sterilized to remove impurities. Table 1.2 shows the components for two types of batch media investigated denoted as media A and B.

Table 1.2 Batch Media Recipes (1 liter)

Component	Media A	Media B
Glycerol	20g	30g
Phosphoric Acid, 85%	26.7 ml	-
Calcium Sulfate	0.93 g	-
Potassium Sulfate	18.2 g	-
Magnesium Sulfate-$7H_20$	14.9 g	1.0 g
Potassium Hydroxide	4.13 g	-
Ammonium Sulfate	-	9.9 g
Potassium Phosphate, pH 6.0	-	50 mM
Potassium Phosphate, monobasic	-	1.9 g
Calcium Chloride	-	0.2 g
Sodium Chloride	-	0.2 g
Biotin	0.8 mg	0.8 mg
Histidine	0.1 g	0.1 g
Trace Metals	6 ml	6 ml

Both medias adjusted to 1 liter volume using deionized water

After adding the batch components, the bioreactor was closed and checked for leaks. The dissolved oxygen (DO) probe, pH probe, and thermometer were all inserted (the pH probe was calibrated using standard 4.0 and 7.0 pH buffers according to bioreactor operating instructions before insertion). The tops of these probes, along with the agitator shaft, were covered with aluminum foil for protection in the autoclave. All ports on the bioreactor were covered with their appropriate cap, clamped shut, and covered with cheese cloth and foil (the exhaust port and one of the media ports were left uncapped and unclamped to allow pressure release during autoclaving). The water jacket was filled with water and then the entire vessel was put into the autoclave for 45 minutes at 121°C (necessary feed bottles and 14 gauge tubing with connectors were also autoclaved).

Following completion of the sterilization procedure in the autoclave, the exhaust port was immediately clamped to maintain the sterile condition and the vessel was connected to the control unit. The thermometer, pH and DO probes were connected to the control unit. An air filter was connected to the sparger port and corresponding air port on the control unit. The external water cooler was connected to the exhaust condenser. At this

point the motor was placed on the agitator shaft and started at 200 rpm, and the control unit air was turned on at 1 volume of air/minute. Once the air was turned on, the exhaust port was unclamped and placed into a graduated cylinder containing water, giving a visual indication of air flow through the bioreactor. Once the temperature of the fermenter cooled to 60°C or below, the water jacket was connected (connecting the water jacket at a higher temperature could result in shattering of the glass vessel) and the temperature was set to 30°C. Also, the remaining media components were added. Prior to inoculation, if the bioreactor was not to be used immediately, the temperature was lowered to 20°C, the condenser port was clamped, and the air source and air sparger were simultaneously turned off.

Prior to inoculation the DO probe was calibrated after a 6 hour polarization period, and the pH probe was re-calibrated after autoclaving. Also, the various set-points for the controls were entered and the data-recording software was started. Table 1.3 summarizes the controls, set-points, and importance of these values for the fermentation.

Table 1.3 Bioreactor Control Set-points for Fermentation of *P. pastoris*

Control	***Set-Point Value***	Importance
Temperature	30°C	Higher temperatures result in lower protein expression, while lower temperatures lead to slow growth
pH	$5.0 \leq$ pH ≤ 6.0	Necessary for growth optimization and secreted protein integrity
Dissolved Oxygen	40%	Maintenance of oxygen levels for metabolic purposes
Agitation	Low = 200 rpm, High = 1200 rpm	Oxygen transfer rate increases with agitation rate; Agitation control is cascaded to DO so that external oxygen can be supplied after agitation has reach maximum
Aeration	$\geq$ 1 volume/min.	Oxygen transfer rate increases with air flow rate

Preparation of Inoculum

For preparation of fermentation inoculum, a 1 ml frozen stock colony was added to a sterile 500 ml shake flask containing 100 ml of sterile BMGH media. The shake flask was then incubated at 30°C and agitated at 300 rpm for about 14 hours, or until the OD measured between 2 and 3 at wavelength 600 nm (inoculation OD measurements were obtained from log phase experiment). The total volume from the shake flask was then added to the vessel containing 1 liter of media via the inoculation port to yield a starting OD between 0.1 and 0.2. The software was synchronized to the time of inoculation.

Batch Phase

The batch phase of the fermentation procedure began with the initial inoculation and was continued until the carbon source, glycerol, was consumed by the growing cells. Because a glycerol probe was not available for this study, glycerol depletion was determined by monitoring the presence of a 'blip' in the DO profile. The initial DO value of nearly 100% decreased to 40% (the set-point), where it was then maintained by the controller by increasing the agitation rate to account for the increased oxygen demand as cell density increased. As glycerol levels were depleted, a quick increase, or 'blip,' in the DO profile indicated that oxygen consumption decreased due to the low glycerol concentration.

Fed Batch Phase

Upon depletion of the glycerol content in the initial batch media, the fed batch phase was initiated by adding fed batch media to the fermentation vessel. The components of this media are listed in Appendix 1.E.

The fed batch media was pumped into the fermentation vessel through a 14 gauge tube connected to a pump located on the control unit. The feed rate was controlled by a profile based on the predicted growth rate of the cells. Fed batch media was continuously

pumped into the vessel according to the profile until the OD leveled off, indicating that cells were no longer growing. Table 1.4 shows the feed rates and corresponding time points for the profile system utilized.

Table 1.4 Profile for Fed Batch Phase

Time (hour of fed batch phase)	Feed Rate (%)
0	6
3	10
6	16
8.5	23
10.5	31
13	45
14.5	56
16.5	76
18	95
19 and up	100

Feed rates based on 14 gauge tubing and flow rate of 6.1 ml/minute

Induction Phase

Upon reaching the maximum cell density, the fed batch media pump was turned off and the cells were 'starved' until the culture was again depleted of glycerol. Once this event occurred, the induction media was pumped into the fermentation vessel. Components of this media are listed in Appendix 1.F.

Two different feeding modes were studied for the induction phase. In Method A, the feed rate was manually controlled by either increasing or decreasing pump speed in order to maintain a constant DO at 40%. In Method B, the feed rate was entered into the control unit under a profile system in the same manner as the fed batch profile. The feed rate percentages for the induction profile of this second method are listed in Table 1.5. Induction feed was allowed to continue depending upon the ability to maintain both DO levels and OD measurements.

Table 1.5 Profile for Induction Phase

Time (hr of induction phase)	Feed Rate (%)
0-2	1
2-4	2
5 and up	3

Feed rates based on 14 gauge tubing and flow rate of 6.1 ml/minute

Samples were taken during the induction phase at 12 hour intervals for a duration of 60 hours to examine recombinant protein expression. The OD was measured approximately every 2 to 5 hours. A 1 ml sample was taken for further recombinant protein analysis using staining and blotting techniques. The 1 ml samples were centrifuged at 4500 rpm for 5 minutes using a Lanet Hermel benchtop centrifuge (model Z 233 M-2) in order to separate the pellet from the supernatant. A 10 ml sample was taken for purification purposes. The 10 ml samples were centrifuged at 4500 rpm using a different model of the same centrifuge instrument (Z 383 K), however, the larger volume required 10 minutes of centrifugation. Both the pellets and supernatants were stored separately at -80°C for further analysis.

Harvesting

At the end of the fermentation, the vessel was cooled to 20°C. The cell broth was then manually pumped out using 16 gauge tubing into Nalgene® 500 ml centrifuge bottles with sealing caps. The bottles were centrifuged to separate the cells and broth at 4500 rpm for 25 minutes at 4°C using a Beckman J2-HS centrifuge. Pellets and supernatants were stored separately at -80°C.

Total Protein Concentration

The total protein concentrations from both the supernatant and pellet fractions were determined using Pierce's BCA™ Protein Assay Kit. This method required that the samples be mixed with a specific amount of BCA (bicinchoninic acid) for the colorimetric detection and quantification of total protein. The protein in the samples reduce Cu^{2+} to Cu^{1+} (Biuret

reaction) using a reagent to detect the reduced cuprous cation. The protein concentrations were determined by comparing them with a standard curve that was generated according to protocol from known protein concentrations of bovine serum albumin (BSA).

Intracellular Protein Extraction

After being thawed the pellets were resuspended in binding buffer (Appendix 1.G). This buffer was used for cell extraction because of its high pH, which would allow the elimination of the pH equilibration step in the purification method to be discussed in Chapter 2. A French press was used at 20,000 psi to break open the cells. The broken cell solution was then centrifuged at 4500 rpm for 5 minutes to remove the insoluble cell debris. The supernatant fraction was then heated for 20 minutes at 80°C to precipitate native yeast proteins, which were then removed by centrifugation.

SDS-PAGE

After being thawed, 20 µl of each supernatant and cell debris sample were mixed with an equal volume of sample buffer (Appendix 1.H). These samples were then heated at 95°C for 5 minutes in order to denature the protein (disrupt secondary and tertiary structures). Each sample (20 µl) was loaded onto "4-20%" Precise ™ protein gels from Pierce Biotechnology, Inc. In addition to the samples, 10 µl of the molecular weight marker Kaleidoscope from Bio-Rad Laboratories was loaded onto each gel. Positope™ from Invitrogen was used as the positive control and was loaded in 10 µl (25 ng) sample sizes for each gel. The Positope™ recombinant protein was engineered with the *c-myc* epitope, so its presence could be detected in Western Blot analysis (Evan, 1985). An external DC voltage power supply was used to send a current through the gels. The running conditions were 120 V for 45 minutes in the presence of running buffer (Appendix 1.I).

Protein Stain

Gels containing supernatant and cell debris samples were analyzed using the protein stain Coomassie® Brilliant Blue R-250 from Bio-Rad Laboratories. The gel was submerged in a generous portion of the stain (~50 ml) and incubated overnight at room temperature while being shaken at 60 rpm. The gel was de-stained using a 4:2:5 ratio of acetic acid, methanol, and distilled water, respectively.

Western Blot

Unstained SDS-PAGE gels were used to analyze the specific proteins by Western Blots. First, the SDS-PAGE gels, along with a Ready Gel™ Blotting Sandwich (0.45 µm nitrocellulose with filter papers) from Bio-Rad Laboratories, and transfer pads were equilibrated in transfer buffer (Appendix 1.J) for 20 minutes. The transfer was conducted using protocols and apparatus from the manufacture (Bio-Rad). The proteins were transferred onto the nitrocellulose membrane for 1.5 hours at 80 volts and 4°C. The membrane was then air-dried and stored at room temperature overnight.

Immunodetection

Each transfer membrane was washed twice using 15 ml of phosphate buffered saline/1% Tween-20 (1X PBST) (Appendix 1.K) at 60 rpm for 5 minutes. Next, the membrane was carefully placed at a 40° angle into a container with 15 ml of blocking buffer (Appendix 1.L). The membrane was incubated in this solution for 1 hour at room temperature at 60 rpm. Following this incubation, the membrane was again washed twice in 1X PBST for 5 minutes. Next, the membrane was incubated with 6 ml of Anti-*myc* antibody, Version D from Invitrogen, which was diluted in blocking buffer to a 1:5,000 concentration. This antibody was specific to the *myc*-epitope engineered at the carboxyl terminus of the recombinant protein. The agitation rate was increased to 150 rpm to assure full dispersion

of the antibody over the membrane, and the incubation period was also increased to two hours. The membrane was again washed twice in 1X PBST for five minutes. Next, the membrane was incubated for one hour in 15 ml of the secondary antibody solution, which was diluted to 1:1,000 in blocking buffer. The secondary antibody was ECL™ anti-mouse IgG horseradish peroxidase linked whole antibody (from sheep) from Amersham Biosciences. The membrane was washed twice in 1X PBST for five minutes before chemiluminescent detection.

Chemiluminescent Detection

Each membrane was placed protein-side up onto a piece of household plastic wrap. ELC™ Western Blotting Detection Reagents from Amersham Biosciences were mixed in equal ratios (1ml: 1ml) and then pipetted onto the membrane and incubated for 1 minute. The membrane was then blotted dry using paper towels before being wrapped in a dry piece of plastic wrap. The membrane was then immediately placed into a light-proof, metal cassette. Three pieces of Hyperfilm ECL™ high-performance chemiluminescent film were placed on top of the membrane. The top two films were developed after 1 hour and 1.5 hour exposure times using GBX developer and fixer from Kodak. The film was developed for two minutes, fixed for five minutes, and then rinsed for one minute in water.

RESULTS AND DISCUSSION

Log Phase Experiment

In the initial stages of growth (lag phase), yeast cells were adjusting the media composition by synthesizing enzymes necessary to grow. Following this period, cells entered into the log, or exponential, growth phase during which the cells divided by binary fission replication. This exponential phase was characterized by a constant rate of cell division. Exponentially growing cells are robust and well characterized, thus inoculation of a

fermenter with these cells results in reproducible growth characteristics in the bioreactor. The results from a representative growth experiment are summarized in Figure 1.2.

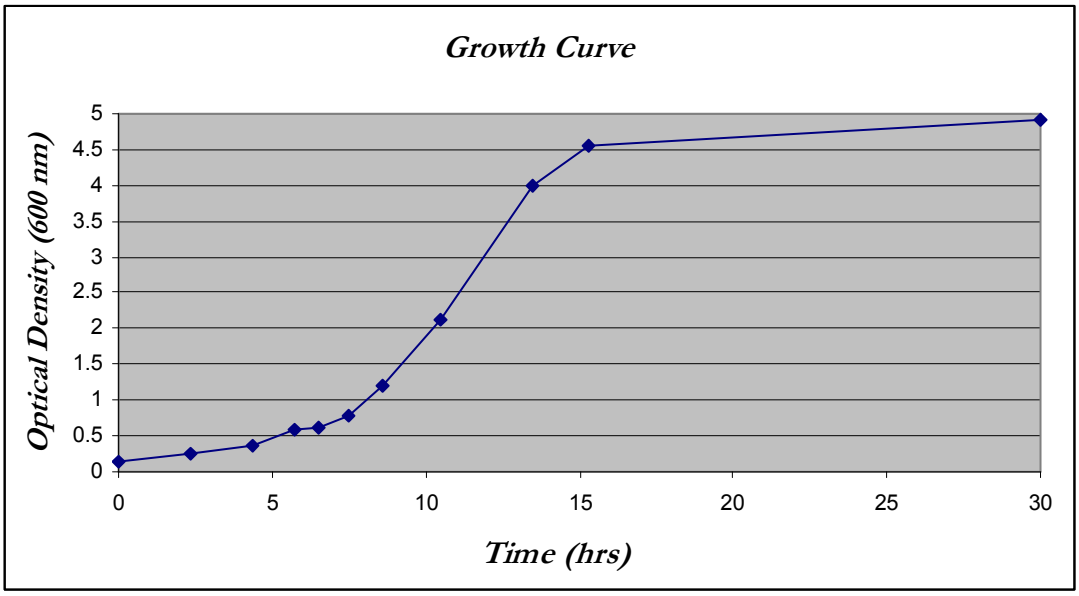

Figure 1.2 Cell Density versus Time for *P. pastoris* GS115 COALA Strain Cultured in a Shake Flask (BMGH Media)

Exponential, or log phase growth occurred between OD measurements of 1 and 4 (Figure 1.2). The average of these two readings, 2.5, was selected as the target OD for cells to be inoculated into the bioreactor.

Batch Media

Two different types of batch media were examined in this study for the COALA yeast strain. Batch media A was based on Invitrogen's basal salts media recipe for *P. pastoris* fermentations. The only altered component of Invitrogen's media was the glycerol concentration, which was lowered from 40 grams to 20 grams in order to decrease the batch time and reduce byproduct accumulation. The yeast cells failed to grow exponentially twelve-hours post-inoculation in this media (+ 0.028 OD) (Figure 1.3). At twelve hours, a second shake flask containing another starter culture in the exponential phase was added to the bioreactor. The cells density immediately increased due to the addition of these cells (+

0.692 OD) (Figure 1.3). The cells were then allowed to continue in the batch phase for another 23.5 hours; however, no significant increase in OD was observed. The culture history data for the fermentation confirmed that the culture was not growing. The DO remained high which indicated that the cells did not need oxygen (Figure 1.3). The DO value within the bioreactor never reached the set-point value of 40% (Appendix 2.A). These cells were viable, however, since cells from the fermenter grew on plates. Thus, the media composition was examined.

Upon further analysis of the media and comparison with the BMGH culture media, nitrogen was found to be the limiting component. Along with carbon and oxygen, nitrogen is a vital nutrient for biological organisms. Nitrogen is necessary for the formation of proteins and nucleic acids. As indicated in Table 1.2, nitrogen was not included in any of the components for Media A. Invitrogen's protocol assumes that sufficient ammonium hydroxide is added to the media at the start of fermentation to raise the pH to the set-point of 5; however, only a small amount of ammonium hydroxide was added to the media to adjust the starting pH from 4.5 to 5.0. Since the initial pH was so close to the set-point 5.0, the cells were only supplied with a small amount of nitrogen which limited cell growth. Figure 1.3 highlights this lack of growth seen in COALA cells under the influence of batch Media A.

In contrast to Media A, Media B contains almost 10 grams per liter of ammonium sulfate as the nitrogen source. In Media B the cell culture grew exponentially for forty hours (Figure 1.3). Additionally, nitrogen was supplied to Media B due to pH control with ammonium hydroxide (Appendix 2.B).

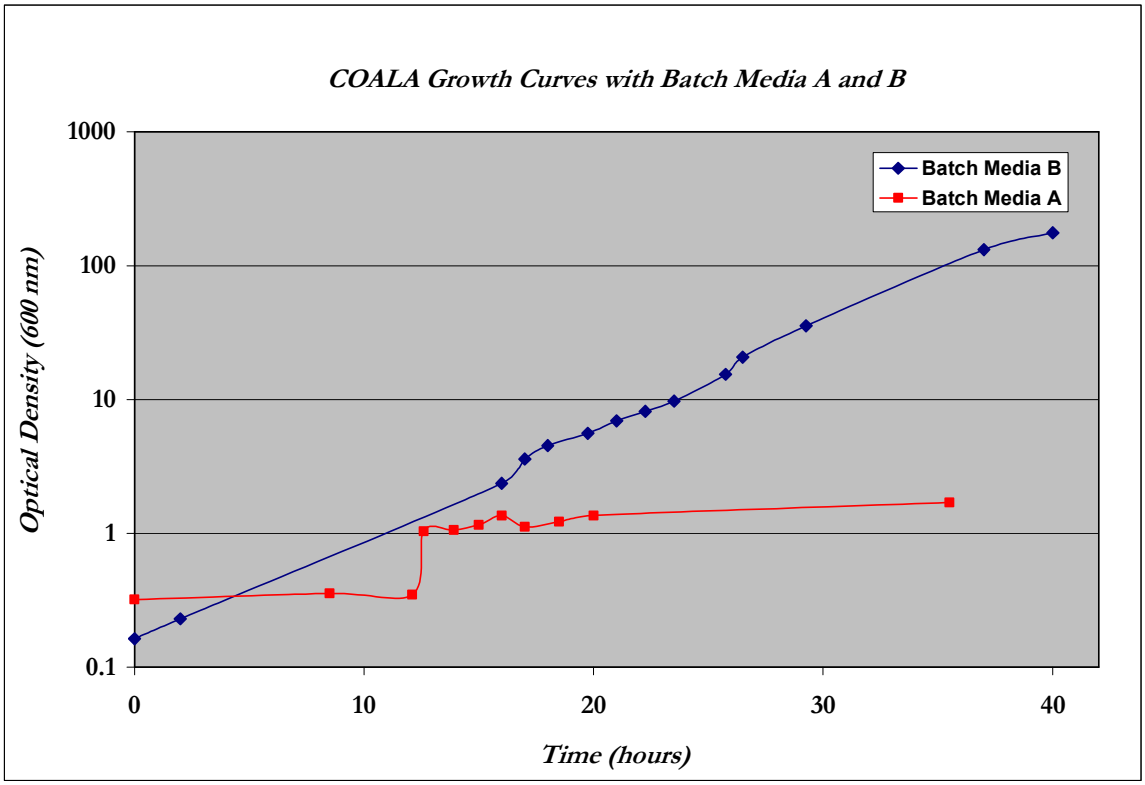

Figure 1.3 Cell Density versus Time for *P. pastoris* GS115 COALA Strains Cultured in a Bioreactor (Batch Media A and B)

Batch Phase

The batch phase growth for the two different clones using Media B, COALA and COLA, showed similar trends. For COALA, the increase in the DO curve occurred at around 25 hours (Appendix 2.C). The increase in the dissolved oxygen levels within the vessel indicated that the cells no longer had a carbon source. The COLA fermentation reached the end of the batch phase at about 20 hours, slightly earlier than COALA (Appendix 2.D). It might appear that the COLA fermentation consumed the same amount of glycerol media in a shorter amount of time due to a higher growth rate, since the starting cell densities were not significantly different (1.35 OD for COLA and 1.63 OD for COALA). The measured growth rate for COLA was about 0.13 h^{-1} during the batch phase and 0.19 h^{-1} for COALA. However, the final cell densities were 5 OD for COLA and 15

OD for COALA. Thus, the COLA strain had a low cell yield on glycerol compared to the COALA strain.

Fed-Batch Phase

The fed-batch phase began after the initial batch glycerol was consumed. A high concentration glycerol fed media was then added to the vessel to increase the biomass. The fed-batch phase continued until the cell density leveled off. At this time, the feed was stopped until the glycerol remaining in the fermentation vessel was depleted, which signaled the start of the induction phase.

For the COALA fermentation, the fed-batch phase began at 25 hours and continued for 17 hours. During this time, 1.9 liters of fed batch media were pumped into the vessel. The feed rate had an exponential trend to promote exponential growth of the cells. The history plot in Appendix 2.G shows that the stir rate was directly proportional to the feed rate which indicates good cell growth. The fed batch growth phase was stopped when the cell density no longer increased as predicted, which was likely due to waste product accumulation. The cells were cultured for an additional 13 hours with no nutrient addition to allow for consumption of any excess glycerol or byproducts. During this "starvation" phase, the cells continued to grow where they reached a cell density of 346 OD. This continued growth in the starvation phase indicated that the cells were overfed during the fed-batch phase and that lower feed rates could be better for these cells. The end of this starvation phase was determined by a decrease in stir rate and increase in the DO (Appendix 2.H), signifying no carbon sources were readily available to the cells.

The fed-batch phase for the COLA fermentation was longer than that of COALA. The fed-batch phase began around 20 hours, when cell density was 5 OD. This fed-batch phase was 44 hours long, ending at 64 hours of fermentation time. Like COALA, the

COLA culture was fed about 2 liters of fed-batch media. The feed profile for COLA was not exponential. The feed profile was manually controlled based on the stir rate (Appendix 2.I). Again, the cells continued to grow in the starvation phase, metabolizing glycerol and waste byproducts for another 26 hours (90 hours fermentation time). Similarly to COALA, the cells density increased in the starvation phase to 280 OD.

Induction Phase

The induction phase began at the end of the starvation phase. For COALA, the induction media feed rate was manually controlled (method A) by turning the methanol pump on and off, at varying rates, depending upon the ability to maintain 40% DO (Appendix 2.J) During this phase, the cell density decreased to 250 OD initially and was maintained at this level until the end of the fermentation. The induction phase lasted for 60 hours and was terminated when the cells were no longer consuming oxygen as indicated by increasing DO levels.

For the COLA induction phase, method B was employed which used a set feed profile (Table 1.5). The induction feed rate increased linearly from 1% to 3% over 4 hours and then remained at 3% for the duration of the induction phase (Appendix 2.K). During this phase the cell density reached a maximum of 350 OD. The stir rate reached its maximum limit of 1200 rpm and supplemental oxygen was used. At the end of the induction phase, the cell density had decreased to about 250 OD. The entire induction phase for COLA was 53 hours. The culture was terminated when the DO started to increase above the set point which demonstrated that the carbon source utilization efficiency was decreasing.

Total Protein Concentration

Using a BCA™ assay, total protein levels from post-induction were determined for both fermentations from culture broths (Table 1.6). The broth total protein levels were the result of protein secretion, cell lysis, and dilution by the feed medias. The COLA samples had higher extracellular total protein concentrations throughout the induction phase. The high initial protein levels gave an indication of the background levels of yeast proteins in the cell broth. For both COLA and COALA, the recombinant proteins were not secreted in significant quantities into the broth because the total protein levels did not significantly increase, as reported secreted protein levels for *P. pastoris* can approach and exceed 100 mg/ml (Cregg, 1993). Thus, we also harvested the pellets to see if the silk copolymers not being secreted were being made. The total soluble protein concentrations obtained from the pellets were dependent on many factors, such as breakage efficiency and buffer volumes, thus these values can only be used as a means to normalize target protein levels to total protein obtained.

Table 1.6 Total Protein Levels Obtained Post-Induction

COLA Time Post-Induction (hr)	Supernatant	Pellet	***COALA Time Post-Induction (hr)***	Supernatant	Pellet
	mg/ml			mg/ml	
0	13	-	**0**	10	-
12	8.9	18	**12**	8.7	14
24	14	16	**24**	8.2	17
36	18	25	**36**	8.4	8.4
48	17	16	**48**	9.6	17
60	19	13	**60**	9.6	17

Protein Stain

The stained SDS-PAGE gels of the supernatant and pellet samples confirmed the total protein values obtained by the BCA™ total protein assay, as the band intensities correlated with the total protein concentration (Figure 1.4, 1.5) In all of the COLA

supernatant samples, two bands similar in size to the target proteins (30 and 60 kDa) were visible. For COALA, two bands of 60 and 100 kDa were most prominent. The COLA pellet samples also showed more visible bands at the 30 and 60 kD markers. In the COALA pellet samples, the 60 kD bands were only barely visible, while the 30 kD band was not seen at all.

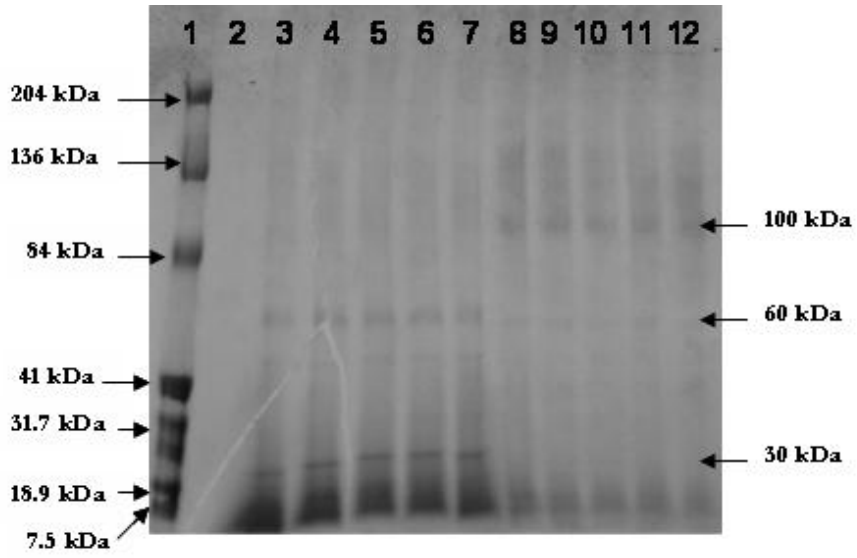

Figure 1.4 SDS-PAGE Gel of COLA and COALA Supernatants: Lane 1 contains the molecular weight marker. Lane 2 contains 25 ng of the positive control protein, Positope™. Lanes 3, 4, 5, 6, and 7 are COLA samples 12, 24, 36, 48, and 60 hrs post-induction, respectively. Lanes 8, 9, 10, 11, and 12 are COALA samples 12, 24, 36, 48, and 60 hrs post-induction, respectively. Equal volumes were (20 µl) loaded in all sample lanes.

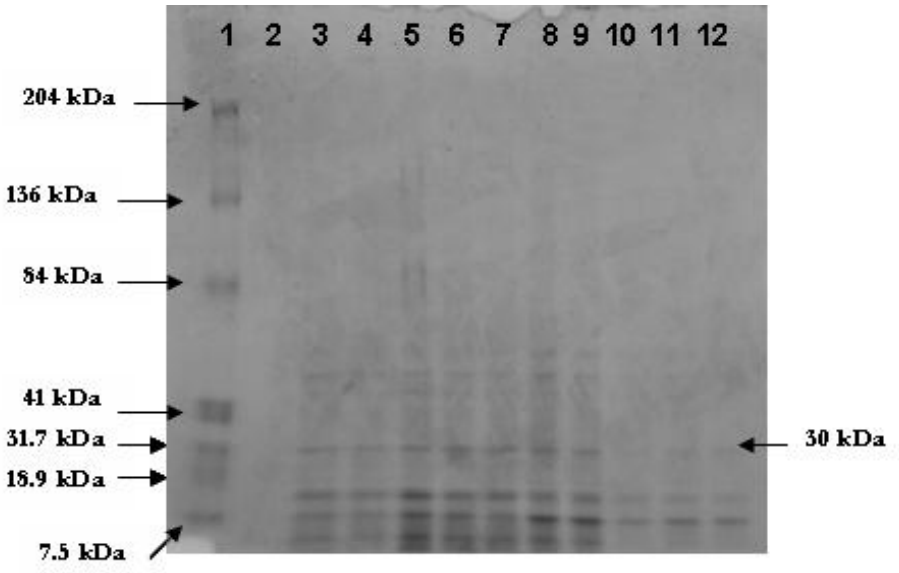

Figure 1.5 SDS-PAGE Gel of COLA and COALA Pellets: Lane 1 contains the molecular weight marker. Lane 2 contains 25 ng of the positive control protein, Positope™. Lanes 3, 4, 5, 6, and 7 are COLA samples 12, 24, 36, 48, and 60 hrs post-induction, respectively. Lanes 8, 9, 10, 11, and 12 are COALA samples 12, 24, 36, 48, and 60 hrs post-induction, respectively. Equal volumes were (20 µl) loaded in all sample lanes.

Western Blot

The results from the Western Blots showed no silk copolymer protein in the supernatant fractions for both strains. Figure 1.6 shows the film after 1 hour exposure time, where only the positive control was seen. The detection limit for the chemiluminescent Western Blot was 2.5 ng/lane which was significantly more sensitive than the Coomassie stain which detected anywhere from 50-100 ng/lane. This difference in detection indicated why the positive control was not be seen in the SDS-PAGE gels. The results from the pellet fractions showed more positive results; however, they still indicated that the expression level of the silk copolymer protein was significantly less than expected. For COALA, the highest amount of the target protein was found in the 12 hour post-induction sample. Therefore, the protein was expressed in the cells soon after induction, but prolonged induction resulted

in protein degradation and no secretion. Further work is necessary to improve the clones prior to additional fermenter optimization studies.

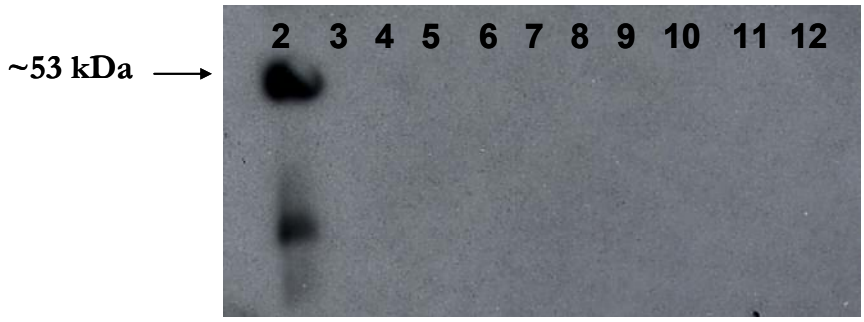

Figure 1.6 Western Blot of COLA and COALA Supernatants: Lane 2 contains 25 ng of the positive control protein, Positope™. Lanes 3, 4, 5, 6, and 7 are COLA samples 12, 24, 36, 48, and 60 hrs post-induction, respectively. Lanes 8, 9, 10, 11, and 12 are COALA samples 12, 24, 36, 48, and 60 hrs post-induction, respectively. Equal volumes were (20 µl) loaded in all sample lanes.

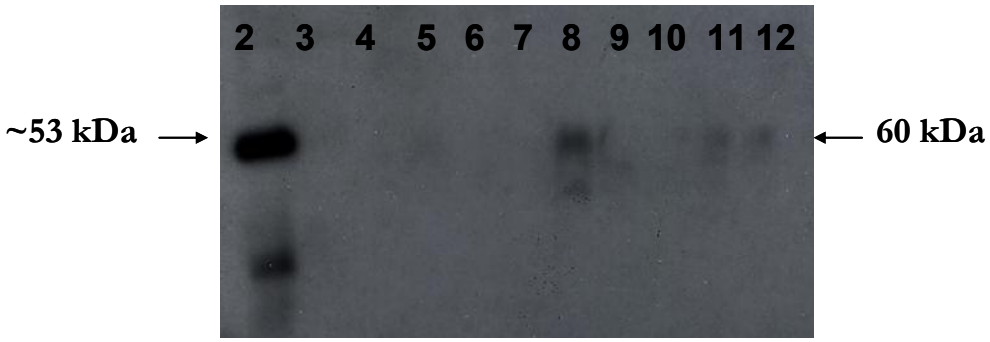

Figure 1.7 Western Blot of COLA and COALA Pellets: Lane 2 contains 25 ng of the positive control protein, Positope™. Lanes 3, 4, 5, 6, and 7 are COLA samples 12, 24, 36, 48, and 60 hrs post-induction, respectively. Lanes 8, 9, 10, 11, and 12 are COALA samples 12, 24, 36, 48, and 60 hrs post-induction, respectively. Equal volumes were (20 µl) loaded in all sample lanes.

CONCLUSIONS

Fermentation optimization of the genetically engineered yeast strains COALA and COLA demonstrated that the cells could be cultured to high cell densities on minimal glycerol media. Without a strong base media, the cells would be unable to proliferate, thereby rendering them incapable of advancing to the final induction phase necessary for protein production. Media A (Table 1.2) was the same as the fermentation basal salts

medium, except for the glycerol concentration, set forth in Invitrogen's fermentation process guidelines for *P. pastoris*. According to their protocol, an undiluted 28% ammonium hydroxide solution should be used to raise the pH to 5.0 before starting the fermentation. This study found several points that contradicted this protocol. First, a large amount of ammonium hydroxide would have to be added in order to supply the cells with enough nitrogen source to obtain the high biomass necessary for the desired level of protein production. Second, the starting pH within the vessel prior to the fermentation was so close to 5.0 that a very small volume of ammonium hydroxide was needed to adjust to the set point. Third, and most notable, high levels of ammonium hydroxide have been shown to have a negative effect on yeast fermentation (Drabble and Scott, 1907). In a study showing the effects various acids, alkalis, and salts had on the fermentation activity of yeast, it was shown that hydroxides not only inhibit fermentation, but small concentrations can have lethal effects by inhibiting reproduction. A study conducted in 2006 also found a problem with Invitrogen's basal salts medium, which has been the most common medium for high cell density fermentations with *P. pastoris*. However, it only alluded to possible problems such as unbalanced composition, ionic strength, and precipitates and was not able to link any results to media insufficiencies (Cos et al., 2006).

The shortcomings exhibited by Media A were overcome by using the benefits of Media B (Table 1.2). This media included an ammonium sulfate component, adding not only a sufficient nitrogen source, but also including a salt ion important for biological functions. Furthermore, the components of this media were responsible for giving a pre-fermentation pH of almost 6.0 (Appendix 2.L). Since a pH value between 5.0-6.0 has shown to be optimum for both growth and recombinant protein secretion (Cregg et al., 1993; Sreekrishna et al., 1997), starting at the maximum limit for pH can be advantageous. This

higher value allows time for the cells to grow and acclimate within the fermentation vessel before reaching a pH of 5.0, a value that initiates the necessary addition of ammonium hydroxide to counteract the increasing amount of acid secreted by the growing cells.

In order to predict the growth rate for a optimal fermentation, the Monod growth model was used. The Monod model is a mathematical representation used to predict the growth rate based on the substrate concentration. It is useful when discussing microbial organism reproduction under cases of slow growth and low population density, all relevant in *P. pastoris* fermentations. Under these conditions for nutrient-limited growth, the following equation is applied:

$$\mu = (\mu_m S)/(K_s + S)$$

where μ = specific growth rate; S = nutrient concentration; μ_m = maximum specific growth rate; K_s = Monod constant, or the concentration of the growth-limiting nutrient at which the specific growth rate is half the maximum value.

Two useful assumptions from this equation can be made. When nutrient concentrations[S] become low, the equation reduces to $\mu = (\mu_m S)/ K_s$, resulting in a linear growth curve. At higher concentrations, the resulting equation becomes $\mu = \mu_m$, giving a horizontal, or stationary, growth curve. Therefore, a lower nutrient concentration results in a higher nutrient affinity. In other words, to obtain an exponential growth for the yeast cells, the feed rate needs to supply only the bare minimum amount of glycerol needed at any given time. Using this information, a common growth curve for yeast growth can be formulated that is used to predict optimum growth (Figure 1.9). With the feed profile listed in Table 1.4, this characteristic growth pattern was obtained in the COALA fermentation (Appendix 2.G).

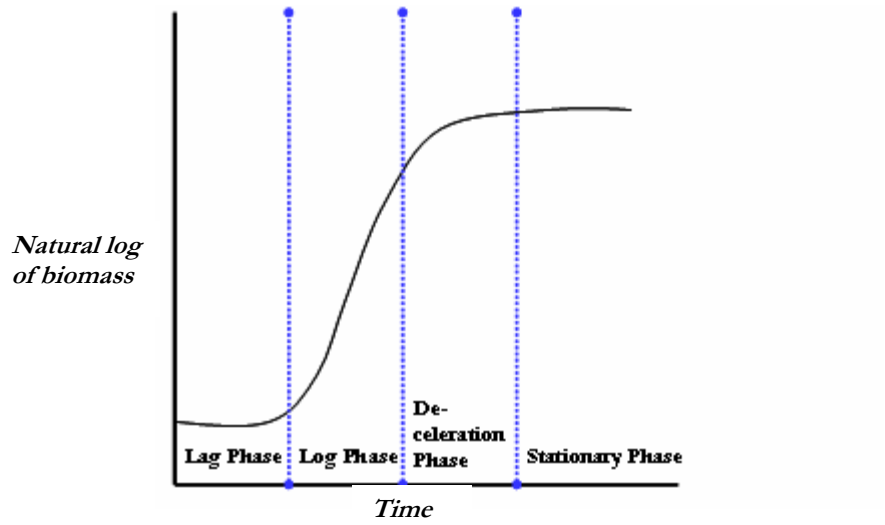

Figure 1.8 Characteristic Growth Curve for Nutrient-Limited Bacterial Growth

In addition to the batch media and feed profiles, strides in optimization were also made during the induction phase. Many published protocols for *P. pastoris* fermentations that call for a 50% glycerol feed solution suggest a 30 minutes to 1 hour period of starvation before inducing the cells with methanol feed ((Cino, 1999), (Cos et al., 2006),). These short periods of starvation are thought to allow time for the cells to consume the remaining glycerol concentration, preventing negative inhibition on the AOX1 promoter (Invitrogen). However, this study showed that in fermentations of both COALA and COLA, the cells continued consuming glycerol and growing in numbers for 13 and 26 hours, respectively, after turning off the feed pump. In fact, it was this long period of supposed 'starvation' that allowed the cells to reach such high cell densities (>200 OD). It is hypothesized that the feed profile may have overfed the cells, but not excessively, such that the cells were able to grow efficiently in a nutrient-limited environment, where they used the remaining glycerol stock to continue this growth pattern once the feed pump was stopped.

The most favorable method of supplying methanol during the induction phase was not determined during this optimization study, because insufficient silk copolymer was made. However, based on cell health, the methanol feed profile (Table 1.5) used in the

COLA fermentation yielded two positive results not obseved in the manual method used in the COALA fermentation. In comparing the history plots in Appendix 1 (J, K), the pump method created a more controllable DO level throughout the induction phase. More notable, however, is the fact that this methanol feed profile also enabled the cells to continue growing during the induction phase. The manual method for COALA simply allowed the cells to maintain their OD around a value of 250. Once the COLA cells adjusted to the presence of methanol, they were able to increase from an OD of 280 to an OD of almost 330 under these stable conditions. This result was important considering a fluctuation in DO anywhere between 2% and 3% can be detrimental to the fermentation process and prevent high cell densities (Cohen, 2006).

In terms of protein production, the majority of the recombinant protein was kept intracellularly instead of being secreted into the supernatant. Also, the Western Blots revealed that the COALA fermentation produced the majority of the protein. However, these results do not imply that COALA had the ability to produce more protein than COLA did. Even though both of these fermentations yielded a cell density of around 350, they achieved these densities at different points during the induction phase. Also, each strain was subjected to different feed rates which influenced the production of recombinant protein. In order to conclude that one strain produces more target protein over the other, each must be subjected to similar fermentation conditions where the optimization parameters from this study are combined.

CHAPTER TWO

Small-Scale Concentration and Purification of Silk/Collagen Recombinant Protein from P. pastoris

BACKGROUND

Cloning techniques have made synthetic protein production a reality; however, the advancement of biotechnology in this field has been dependent upon the successful completion of subsequent purification and concentration methods (Amersham, 2001). Fortunately, with the completion of the human genome project and the developing science of proteomics, researchers are focusing on the area of protein purification now more than ever. This demand is only further increased with the pressures placed by cancer, diabetes, and Alzheimer's research which requires pure protein for drug development. Therefore, progress is being made to meet the needs that a rapidly-growing recombinant industry requires (Ghosh, 2003; Smith, 2005).

Protein purification is a necessary component in industries such as biotechnology and the food industry for a number of different reasons, such as removal of impurities, prevention of catalysis poisoning, recommended product specifications, enhancement of protein stability, and reduction of protein degradation. Unfortunately, the isolation and purification of protein from biological sources is widely known to be an extremely challenging process, both technically and economically (Ghosh, 2003). Proteins produced in bioreactors must be separated from the host associated proteins, nucleic acids, and cell debris using removal, isolation, purification, and polishing steps. RIPP is a common acronym which stands for these four basic steps. A confounding factor regarding the

purification of recombinant proteins is that the product is often produced in extremely dilute solutions (Belter, 1988).

Chromatography is a common purification method used to separate proteins (Smith, 2005). Chromatography separates the target proteins from other components using a stationary phase intended to adsorb the desired protein. A commonly used technique is column chromatography where the stationary phase is packed into a column. The solution containing the desired product is then passed over the column and the target protein interacts with the stationary phase such that many of the impurities exit the column. Many chromatography stationary phases exist that allow selection of characteristics unique to a specific protein to be leveraged. Common chromatography methods are ion exchange, reverse phase HPLC, size-exclusion, and affinity chromatography which includes metal and immuno-affinity (Ghosh, 2003).

Incorporation of peptide tags into a recombinant protein have enabled chromatography purification of various target proteins based on the peptide tag (or affinity tag) (Hengen, 1995). One example is the his-tag, a 6-mer of histidine residues. The his-tag has an affinity for ions such as Cu^{2+}, Ni^{2+}, Co^{2+}, and Zn^{2+} that allow it to be purified from other proteins using metal affinity chromatography, which has been shown to have up to 95% yields (Hochuli, 1988).

Ultrafiltration is a technique that uses membranes and high-pressures to separate molecules based on size or molecular weight (Lo, 1996). Furthermore, its ability to separate impurities and bacteria in addition to being able to isolate proteins has made it applicable to the chemical, biotechnology, pharmaceutical, and food industries (Cheryan, 1998). Ultrafiltration of recombinant proteins allows for the removal of water and some removal of host proteins. For yeast fermentations, ultrafiltration can be a purification tool to remove

water because of the tendency of yeast to secrete the recombinant proteins and not native proteins (Sun et al., 2006).

The step-wise purification process outlined above involving preliminary cell extraction and centrifugation, chromatography, and ultrafiltration steps is currently the most popular method of isolating and purifying proteins (Chang, 1996). However, this system is plagued with several problems that can be detrimental to the protein and costly to the producer. Each of these steps is necessary in order to safely remove contaminants and impurities; unfortunately, the use of multiple steps leads to protein loss, greater operational costs, and longer processing times (Charoenrat, 2005). It is possible to reduce the number of purification steps if measures are taken beforehand to carefully combine operations and select the ones that are absolutely necessary (Roy, 1999). Not only do cell extraction and centrifugation methods increase the processing time, but they also expose the recombinant protein to many soluble byproducts which have the potential to degrade the desired product (Anspach et al., 1999). In addition, these byproducts may hinder purification methods such as chromatography which require particle-free solutions. Ultrafiltration removes water well, but can be expensive to operate and may cause precipitation problems for certain proteins (Bailey, 2000). Solutions to these obstacles, such as expanded bed adsorption process (EBA), have shown potential for recovering recombinant protein from crude feedstock materials (Hyjorth, 1997). This system reduces cost, time, and product loss by combining the purification and concentration steps into one operation utilizing an absorbent column with crude-cellular material being pumped in (Curbelo, 2003). In fact, recent studies have shown it to be an effective and even more efficient system for the initial isolation of target proteins (Charoenrat, 2005).

This chapter investigates the use of ultrafiltration and chromatography as means to purify the silk copolymer. The silk copolymer samples were obtained from small-scale expression experiments of the COLA strain. The silk copolymer protein levels at various purification steps were qualitatively determined by Western Blots.

MATERIALS AND METHODS

Small-Scale Expression

The yeast cells were cultured according to Invitrogen's *Pichia* Manual. COALA and COLA yeast cultures were first colonized onto YPDS (Appendix 1.A) plates using the same procedure discussed in the Materials and Methods section from Chapter 1. From these cultures, 250 ml baffled shake flasks containing 25 ml of BMGH (Appendix 1.B) were inoculated with a single colony. The flasks were incubated at 30°C and at 300 rpm until the cell culture reached an OD value ranging between 2 and 6. After 17 hours of growth, the COALA and COLA strains were in exponential growth at around 4 OD. These cultures were then centrifuged at 3000 rpm for 3 minutes using a Lanet Hermel benchtop centrifuge (model Z 383 K). Cell pellets were resuspended in 89 ml of BMMH media (Appendix 1.M) to achieve a final OD of 1. Methanol (100%) was added to the shake flasks every 24 hours to maintain a 0.5% concentration. After 70 hours of induction at 30°C and 300 rpm, the cultures had reached cell densities of around 10 OD. Supernatants and pellets were separated at 4500 rpm for 5 minutes and stored at -80°C.

Concentration

The supernatant was thawed and processed using an Amicon 400 ml stirred cell from Millipore (model #8400) with 100 kDa and 10 kDa regenerated cellulose ultrafiltration discs (catalogue No. PLHK07610, catalogue No. PLGCO7610) (Figure 2.1). The first filtration used the 100 kDa membrane, which should allow the silk copolymer solution to pass

through. The filtrate from the first step was then added to the Amicon stirred cell with the 10 kDa membrane. For this membrane the silk copolymer protein should be retained in the stirred cell (retentate) while smaller proteins (< 10 kDa) and water are removed. Instructions from Millipore were followed to operate this device.

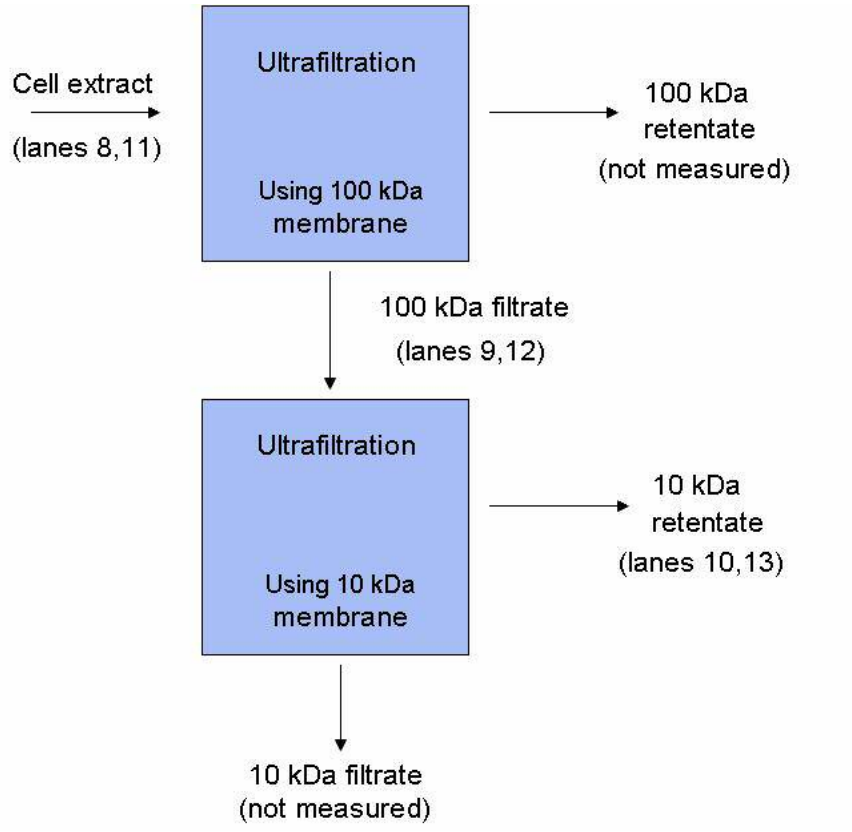

Figure 2.1 Flow Diagram for Ultrafiltration Process of Cell Extracts from *P. pastoris* GS115 COLA and COALA Strains. The pore sizes of the membranes used in the steps were 100 kDa and 10 kDa, respectively. Samples were alalyzed by SDS-PAGE and Western Blots shown in Figures 2.2 and 2.3 and correspond to the lane numbers given for each step.

Purification

The COLA pellets were thawed and then vortexted to resuspend the cells in breaking buffer (Appendix 1.N). This total volume was then passed through a French press at 20,000 psi for two cycles. The disrupted pellets were then centrifuged at 4500 rpm for 5

minutes to remove insoluble cell debris. The crude cell extract was then heated for 20 minutes at 80°C to precipitate native yeast proteins and then re-centrifuged to obtain the soluble cell extract.

In order to purify the silk copolymer protein, the cell extract was first brought to pH 8.0. The sample was loaded into a dialysis bag and then submerged in binding buffer solution (Appendix 1.G) until the pH reached 8.0, which was determined using pH paper.

Affinity chromatography was used to purify the silk copolymer protein. First, glass fiber was placed into the bottom of a 50 ml syringe and then the Nickel-NTA HisBind resin (the affinity resin) from Novagen (catalogue # 70666) was packed into the syringe to give a bed volume of 25 ml. Binding buffer (125 ml) (Appendix 1.G) was loaded onto the column and allowed to flow by gravity. This step equilibrated the resin.

The pH-adjusted cell extract was loaded onto the equilibrated resin column and again allowed to flow through by gravity. Next, 125 ml of Wash 1 buffer (Appendix 1.O) was loaded on the column, followed by 125 ml of Wash 2 buffer (Appendix 1.P). The silk copolymer was eluded using 75 ml of Elution 1 and Elution 2 buffers (Appendix 1.Q, 1.R). Each wash and elution from the column was saved and stored at 4°C for later analysis.

SDS-PAGE

Samples from the ultrafiltration and chromatography column were examined using SDS-PAGE and Western Blots. After thawing, each sample (20 µl) to be tested was mixed with an equal volume of sample buffer (Appendix 1.H). The samples were then heated at 95°C for 5 minutes. Samples were loaded onto "4-20%" Precise ™ protein gels from Pierce Biotechnology, Inc. In addition to the samples, 10 µl of the molecular weight marker Kaleidoscope from Bio-Rad Laboratories and 10 µl (25 ng) of the positive control

Positope™ from Invitrogen were loaded onto the gels. SDS-PAGE and Western Blot procedures are described in the Materials and Methods section of Chapter 1.

RESULTS AND DISCUSSION

Ultrafiltration Concentration

The results from the SDS-PAGE gel of the concentrated supernatant solutions showed two samples with protein, lanes 8 and 11 (Figure 2.2). These lanes represented the 10 kDa retentate from each strain, where the protein appeared to be around 60 kDa. The Western Blot detected silk copolymer in all six samples, lanes 6-11 (Figure 2.3). For each strain, the highest amount of protein was observed in the final retentate; however, the cell extract contained an equal concentration of the target protein. The 100 kDa filtrate samples had the lowest concentrations of target protein. Also, both the COLA and COALA strains showed bands in the final retentate that appeared around 50 kDa.

Chromatography Purification

The SDS-PAGE gel from the purification procedure showed only one sample, lane 7, with any significant amount of protein (Figure 2.2). This sample corresponded to the solution remaining in the column after purification and, although it showed a large amount of protein, no distinct bands were apparent. Also, the Western Blot in Figure 2.3 revealed that none of the target protein was in this lane. The only other lane that detected any protein in Western Blot was the Elution 1 lane; however, it appeared to be an artifact and not an actual band.

An unexpected result was observed during the chromatography experiment. After the sample was loaded onto the column and allowed to flow for a short time, a fiber-like structure formed in the solution on top of the column. The material formed was a very fine, fiber-like strand and is shown in Figure 2.4. The "fiber" ran from the top of the resin bed to

one side of the column wall and immediately disappeared into solution when the column was disturbed. When the solution was further concentrated, another fiber briefly appeared.

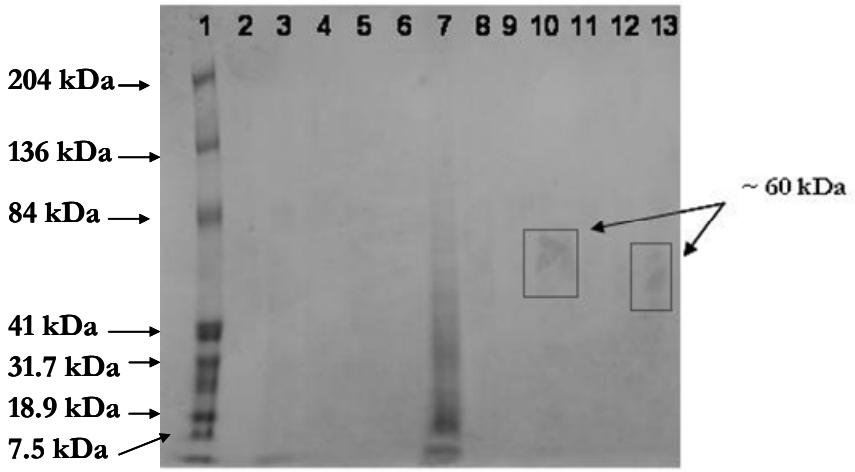

Figure 2.2 SDS PAGE Gel of COLA Column Purified Samples (lanes 3-7) and COLA and COALA Ultrafiltration Concentration Samples (lanes 8-13): Lane 1 contains the molecular weight marker. Lane 2 contains 25 ng of the positive control protein, Positope™. Lanes 3, 4, 5, and 6 are wash 1, wash 2, elution 1, and elution 2, respectively. Lane 7 is a sample retained in the column where fiber formation occurred. Lanes 8, 9, and 10 are COLA cell extract, 100 kDa filtrate, and 10 kDa retentate, respectively. Lanes 11, 12, and 13 are COALA cell extract, 100 kDa filtrate, and 10 kDa retentate, respectively.

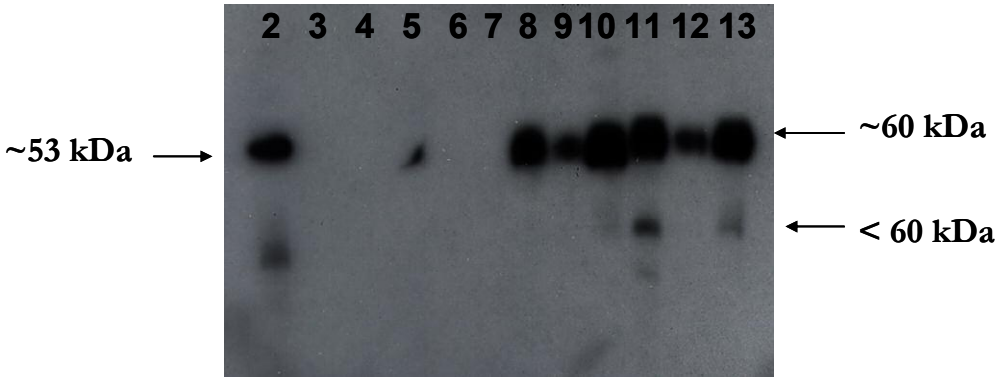

Figure 2.3 Western Blot of COLA Column Purified Samples (lanes 3-7) and COLA and COALA Ultrafiltration Concentration Samples (lanes 8-13): Lane 2 contains 25 ng of the positive control protein, Positope™. Lanes 3, 4, 5, and 6 are wash 1, wash 2, elution 1, and elution 2, respectively. Lane 7 is a sample retained in the column where fiber formation occurred. Lanes 8, 9, and 10 are COLA cell extract, 100 kDa filtrate, and 10 kDa retentate, respectively. Lanes 11, 12, and 13 are COALA cell extract, 100 kDa filtrate, and 10 kDa retentate, respectively.

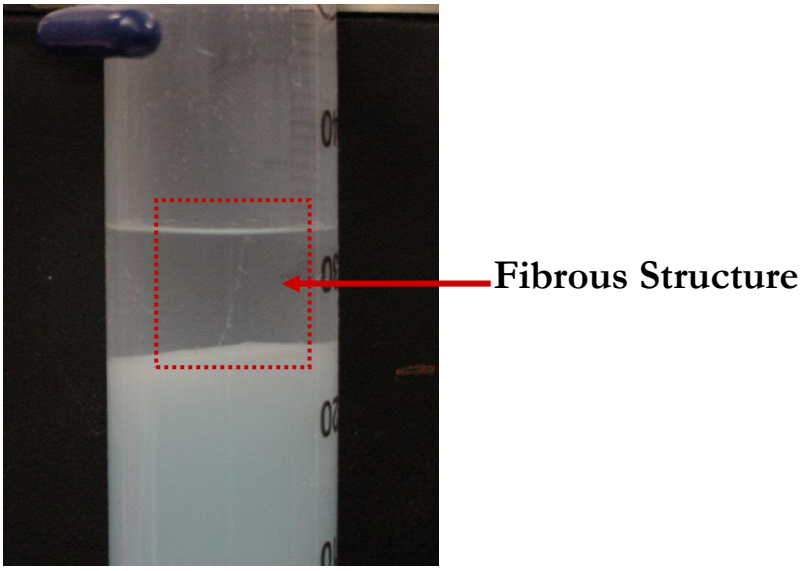

Figure 2.4 Picture of Fiber-like Structure Formed during Column Chromatography Purification

CONCLUSIONS

The SDS-PAGE gel and Western Blot showed that the ultrafiltration method was successful in concentrating silk copolymer protein, however, the level of protein concentrated was small. The Coomassie stain detected 50-100 ng of protein per lane, while the chemiluminscent Western Blot method detected 2.5 ng/lane. Thus, the positive control sample (25 ng) did not show up on the SDS-PAGE gel because it was below the detection limit, but it was seen on the Western Blot. The, silk copolymer protein was detected by Western Blots for both strains in the 10 kDa retentate samples, indicating that the ultrafiltration concentration method was successful in yielding a higher amount of protein by eliminating water and other solvent. However, the Western Blot revealed that the cell extracts had almost the same amount of target protein as the 10 kDa rententate samples, indicating a loss of protein to the 100 kDa filtrate. Furthermore, the filtrate samples contained the least amount of target protein, also suggesting that loss occurred during this step.

The column purification of COLA yielded unexpected results. When the cell extract was loaded onto the column, a fiber formed in the fluid above the column stationary phase. If the fiber was the silk copolymer protein, it appeared that the presence of the resin, Nickel, or both can cause the silk copolymer to self-assemble. The assembly process may also be concentration dependent. Additionally, the high pH of the loading buffer may induce the fiber-formation. Further studies are needed to determine if the observed fibers are the silk copolymer protein. If so, additional studies are needed to determine what specific conditions are necessary for fiber self-assembly. These results would allow for control of the fiber self-assembly process.

CHAPTER THREE
COMPARATIVE STUDIES WITH NATURAL SPIDER SILK

BACKGROUND

Orb-weaving spiders are excellent models for creating novel fibers. Their silk not only mechanically out-performs any natural fiber in terms of tensile strength and toughness, but it is also comparable to many of the synthetically produced fibers in use today (Gosline et al., 1999). Therefore, much work has been conducted to gain a better understanding of the design of these materials. However, according to well-known silk researchers, such as Gosline and Wainwright, these efforts will be futile unless measures are taken to identify the relationships between structure and function of silk (1999, 1988). Gosline points out that much of the research into silk structure has used *Araneus diadematus* silk, while more of the functional-type studies have used *N. clavipes* silk, a discrepancy that has the potential for future problems if research into both these species is inadequate or misrepresented (1999). Until mechanical properties can be directly correlated with function, the design of the already known sequences and protein structure will continue to be a major obstacle for the genetic engineering of spider silk.

One way to understand these structure-function relationships is to first look at spiders and the ways in which different processing conditions influence the nature of their silk. The conformation of silk does not solely rely on the initial molecular structure, but is also influenced by the spinning conditions and other processes affecting the deformation history. Work completed by Pan et al in 2004 has shown conclusive evidence that the molecular make-up of spider silk is not solely responsible for the mechanical properties

exhibited by natural silk fibers. The spiders themselves are able to control the properties depending upon various environmental conditions and impart different molecular orientations depending on habitat and intended use. Looking at how the spiders alter the mechanical and molecular properties of their silk in response to various environmental fluctuations will provide much-needed insight into designing silk's genetically-engineered counterpart (Pan, 2004).

Pan et al. was able to correlate spinning conditions of the spider with mechanical properties of the silk. The spiders used in the study were *A. ventricosus*, orb-weavers native to Korea. Raman Spectroscopy and electronic tensile testing measurements revealed varying amounts of β-sheet and α- helical formation depending upon the manner in which the samples were collected. The first two of these samples were obtained from a spider that rappelled from a 100-cm high platform and then from one that was artificially silked at a constant speed. The latter two samples were collected directly from the spiders' living chambers, one being a 5-cm high carton and the other a 35-cm high glass box (Pan, 2004).

The Raman spectra of samples were measured using laser beams polarized both parallel and perpendicular to the fiber axis. The conformations of the polypeptides observed from the four samples consisted of a majority of β-sheet and α-helix structures in conjunction with random coil and β-turn structures. However, the distribution of these molecular structures varied among the samples. The peak at 1667 cm^{-1} represented the C=O stretching of the amide I and was indicative of β –sheet formation. This peak varied among the different spinning conditions and was most intense in the silk of the spider which rappelled, where there was the highest degree of orientation acting in proportion to the spider's weight and dropping velocity. The silk that was reeled showed the second highest amount of β-sheet orientation. Most surprisingly was that there was a notable difference

between β-sheet orientation among the two spiders in a 5-cm carton and a 35-cm glass container. The 35-cm glass container sample showed the higher amount, which according to the researchers, implied that the molecular structure was influenced by the security of the spider's environment. It was therefore inferred by these researchers that when a spider is confronted with danger, spinning mechanisms adjust (i.e. tensing of muscles) in order to create a more oriented fiber. Therefore, in order to reproduce a fiber that mimics the properties of silk, it will be necessary to thoroughly study and understand the spider's spinning apparatus (Pan, 2004).

Pan et al. also showed that correlation exists between α-helical structures and spinning conditions. The characteristic Raman peak was 1650 cm^{-1} for the spider reared in the 5-cm carton and was not observed clearly in the dragline of the dropping spider. There was also an increase in strength and initial modulus with reel velocity, indicating that speed was necessary for the stretching and subsequent orienting of the molecules. An increase in amount of random coil structures was observed proportional to an increase in environmental security. To summarize, both the spinning conditions and environment had notable effects on the conformation of the dragline silk. Molecular orientation increased in the silk under more dangerous environments. The mechanical properties tested also correlated with their results. Additionally, the highest strength and toughness were observed for the dropping spider. The breaking stress and toughness were lower when environmental safety increased. The results provided by this study demonstrated that an understanding of the spinning conditions and environments under which silk is produced could lead to an improvement in the technology for mimicking the properties of dragline spider silk (Pan, 2004).

Another recent study, by Y. Yang in 2005, highlighted the inter-relations between structure and function in regards to temperature dependence. Climate and temperature have been shown to strongly affect silk and web-building behavior (Foelix, 1996). Because spiders are ectotherms, they rely on external heat to raise their body temperature and seek out cooler environments if their temperature becomes too high. Therefore, spider silk must be able to function under a wide variety of temperatures. Using this information, Yang et al. concluded that spider silk has evolved to remain intact and useful under the temperature rang 0°C to 60°C. This conclusion brought about further investigations into what happens to silk when exposed to temperatures outside of this range (Yang, 2005).

Yang et al. used dragline silk from *N. edulis* and examined its performance from -60°C to 150°C. Data revealed that at high temperatures, the silk behaved like most other polymeric materials, in that its tensile strength decreased. The elongation at the break point for silk however, decreased with increasing temperature, a property that is highly unusual for high-performance fibers. A decrease of temperature surprisingly showed an increase in both strength and the elongation at the break point. In addition, when the silk was broken in liquid nitrogen (-196°C), the silk showed evidence of stretching at the fracture. Unlike other polymeric materials, spider silk fracture is ductile and tough at extremely low temperatures (Yang, 2005).

These temperature study results led Yang et al. to hypothesize a new molecular model for spider silk to explain the functions observed. They first revised a previously proposed model in which silk was a matrix comprising unordered amorphous, rubbery chains reinforced by crystal structures (Termonia, 1994). The new model incorporated two relaxation peaks which were observed at 198°C and 290°C using a dynamic mechanical thermal analyzer (DMTA). Below 198°C, their model showed that non-crystalline parts of

the silk aligned with the fiber axis and were held together through hydrogen bonding. Above 198°C, the hydrogen bonds were broken which resulted in a more rubbery configuration with a crystalline portion. This model helped explain the high storage modulus seen in DMTA studies when temperatures increased from 198°C to 290°C. The temperature dependence behavior of spider silk has the potential to introduce new properties into high-performing fibers of the future, in particular superior performance under harsh environmental conditions (Yang, 2005).

A similar study into temperature-property relationships was conducted by a group led by Manual Elices (2005). Their work on *Arigiope trifasciata* found similar behavior with regards to temperatures, and also examined a new parameter, humidity, to better understand silk properties. They observed that both an increase in temperature and humidity caused a decrease in the initial elastic modulus, yield stress, and overall slope of the stress-strain curve. Like Yang et al., they concluded that this behavior was the result of disruption of the hydrogen bonds, which produced fibers with more elastomeric behavior. More interestingly, their work went on to observe this hydrogen bond phenomenon in regards to the natural spinning process of the spider (Elices, 2005).

Elices et al. began correlating temperature and humidity with silk properties by examining silk formation from aqueous, concentrated protein solutions. In the spider, there are several structures along the duct and the spigot of the spinning apparatus that appear to be responsible for eliminating water from the aqueous solution. Basing their hypothesis on the assumption that the water concentration is a vital component in spinning, they exposed the silk fibers to water baths and observed the reactions. The major ampullate silk fibers underwent a reaction known as supercontraction, where the fibers shrank more than 50% of its original length and underwent drastic mechanical changes. These supercontracted fibers

showed a low elastic modulus but high strain at break, accompanied by a higher modulus once dried (Elices 2005).

Next, Elices et al. went on to compare the contraction of the fiber with stretching in order to find a potential biological explanation. They subjected silk fibers to a process known as wet stretching in which silk was allowed to supercontract in a water bath, stretched, and allowed to dry. This process in theory forced the disruption of hydrogen bonds by the presence of water molecules and then stretched the material more, creating new hydrogen bonds which were locked into place after the drying step. This study showed that this process, known as wet stretching, could account for the whole range of tensile properties exhibited by spider silk. Thus, a similar sequence of events within the silk gland would account for the spider's ability to modify mechanical properties according to the intended use. The fact that these stretching and contracting practices expend only a minimal amount of energy further supports their conclusion. These studies have provided useful information from which to build upon, and also given hope in one day designing an engineering-grade fiber that can convert into a reusable material just by subjecting it to a wet-stretching process (Elices, 2005).

Studying the ways in which spiders modify the properties of silk has begun and will hopefully continue to increase our understanding of this process such that improved synthetic silks can be economically developed. A 2005 study by Liu et al. has already built upon one of the principles discussed. Their research using *N. clavipes* showed that dragline silk spun into a water batch extended the wet-spinning phase, imparting more molecular orientation and increasing the stiffness and resilience of the fiber. Thus, their experiments demonstrated that it may be possible to vary the mechanical properties of the silk by either increasing or decreasing the length of the wet-spinning batch, much like the previous

authors believed the spiders change the supercontraction and stretching conditions within their spinnerets. The results obtained from this study provide a useful link between structure and function which may enable new spinning processes to be developed for synthetic silks (Liu, 2005).

Chapter 3 describes comparative studies that focus on the temperature fluctuations observed in the spinneret region of *N. clavipes* during silk collection. Images were captured by silking spiders under a thermal imager. Thermal pictures were also obtained from non-silked spiders for comparison.

MATERIALS AND METHODS

Maintenance of N. clavipes Spider Farm

Spiders of the species *N. clavipes* were collected for the purpose of comparative studies. Spiders were obtained from two separate locations. Some of the spiders were raised in a green house by biologist Jackie Palmer in North Carolina. Once the spiders reached maturity, they were sent to Clemson University in Clemson, SC to be raised in captivity. Mature spiders were also collected was from Charleston, SC.

At Clemson, spiders were housed in a mesh tent measuring 9 feet in width, 7 feet in length, and 6 feet in height, totaling 378 ft^3 (Appendix 3.A). Each spider required at least 25 ft^3 for peaceful cohabitation, as less space resulted in carnivorous behavior. *N. clavipes*, as well as all spider species, are extremely territorial in nature and will tend to provoke a fatal dispute if their web is intruded (Riechert, 1978).

The tent was housed in a multi-purpose room on the campus of Clemson University. The temperature in the tent was approximately room temperature (~25°C). Humidity was controlled using a standard, household electric humidifier which was operated with deionized water.

Strings were hung inside of the tent in a grid-like fashion (Figure 3.1). This pattern enabled easy release of the spiders once they were either brought in from the field or finished silking. The glass jar containing the spider would simply be placed at the bottom of a string, and the spider would be left to climb to the top of the tent to build a web its own. (Appendix 3.B). The strings also proved to be a useful tool in isolating the spiders from one another, since they usually incorporated at least one of the strings into the construction of their web.

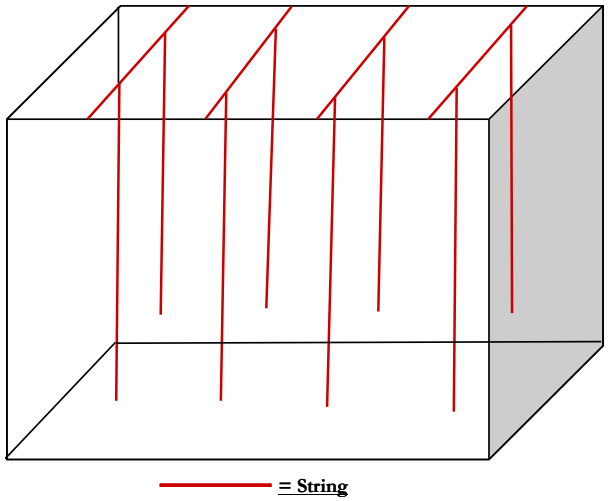

Figure 3.1 Schematic of Spider Tent Containing a Grid-Like Pattern of String

Spiders were misted with deoinzed water from a spray bottle at least once a day. Also, spiders were fed a regular diet of crickets obtained from a local pet supply shop. The crickets' hind legs were removed before placing them in the web to prevent them from kicking their way out of the web or from harming the spider. Spiders were fed anywhere from one to three crickets a day, but on average each spider received one cricket per day. Feeding was usually done in the late evenings because the spiders' nocturnal behavior resulted in quicker response times, allowing the cricket to be captured before falling out of the web (Appendix 3.C). Also, spiders were misted before feeding in order to condition

their behavior. When this technique was done consistently, spiders seemed to expect the cricket which yielded a quicker response time.

Lights remained on inside of the multi-purpose room from approximately 8:00 am-5:00 pm Monday-Friday. Lights were not on during Saturday and Sunday. However, the tent was positioned by two large windows, allowing natural sunlight to penetrate the tent during daylight hours.

Silk Collection

In order to silk the spiders, they were first confined in glass jars and then placed into a 4°C refrigerator until they were in a fully sedated state (~1 hour) (Appendix 3.D). Once they became unresponsive, the spiders were restrained onto their backs (ventral side up) using a piece of Styrofoam and metal staples (Appendix 3.E). The staples were then quickly placed over as many segments of their legs as possible and always over the abdomen, as depicted in figure 3.2.

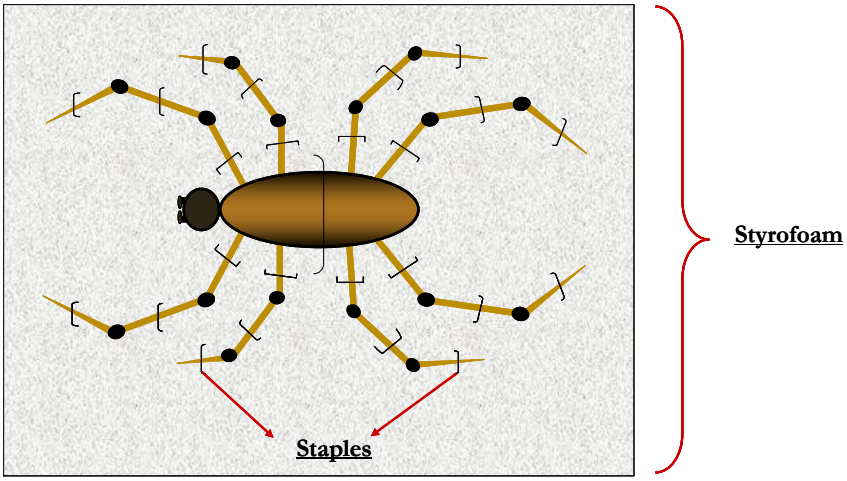

Figure 3.2 Schematic of Spider Restrained on Styrofoam in Preparation for Silking

The spiders were marked for identification once immobilized. A brightly colored, pink nail polish was used to provide a system for recording the spiders as a way of tracking their silkings. Special precaution was taken not to silk the same spider too often or on

consecutive days. This technique helped to reduce the stress placed on the spiders, thus helping to increase their lifespan. The spiders would periodically molt their exoskeleton, eliminating the marking left by the polish. If molting occurred, the spider was either re-marked with the same identification if known, or if not known, the spider would be given a new marking. A drop of the nail polish was placed on one of 12 places: one of the three segments on either the front or back pair of legs. The diagram in Figure 3.3 shows this system for labeling the legs. In addition to being labeled, the spiders were also measured before each silking. The length of the body was recorded along with the total length from front leg to back leg (Appendix 3.F). Other observations such as whether the spiders were eating regularly and whether they were constructing a normal web were also recorded. These various notes were made and documented in case future studies correlating these parameters and silk properties are to be conducted.

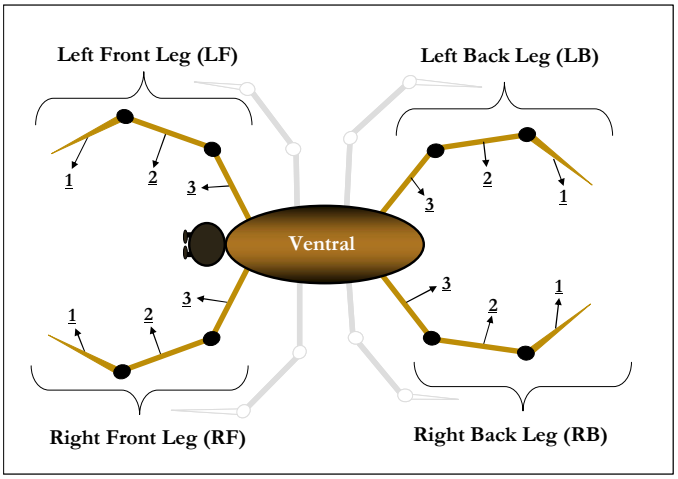

Figure 3.3 System for Labeling Spiders: nail polish was placed on either of the three segments on either the front or back pair of legs.

The silk was collected on a spool constructed of washers and nails. Eight thin nails were evenly spaced along a rubber washer. The rubber washer was then super-glued to a metal washer in order to provide more stability. The winder was constructed by The School

of Materials Science and Engineering's computer technician David White. The electronic device is extremely light weight and small in scale (measuring about 1 foot in length) so it is convenient for table-top use. There are four different speeds on the winder: 0.72 mm/sec, 0.96 mm/sec, 1.57 mm/sec, and 2.16 mm/sec.

The spiders were silked by taking their dragline silk with a pair of tweezers and extending it over the spool until it attached to one of the nails. The spiders were silked at various speeds, again being documented for future studies. It was discovered that an excess of silk on one spool made it difficult to separate strands for Raman spectroscopy and tensile testing. Therefore, spools were changed out during silking too allow for easy sampling. Once collected, the silk was placed into a large pill bottle obtained from a local pharmacy. A bolt was inserted through the lid which allowed the spool to be tightly secured.

While collecting silk, thermal images were obtained using a TH5104 Iroman Thermal Imager from Mikron Instrument Company. The camera was placed above the spider and focused over the spinneret region. Figure 3.4-3.6 shows drawings of the winder, spool, and storage container. Figure 3.7 shows the entire process of taking thermal images while the spider is being silked.

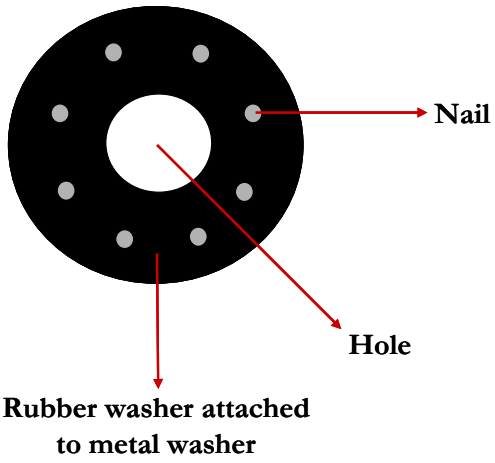

Figure 3.4 Overhead View of Spool

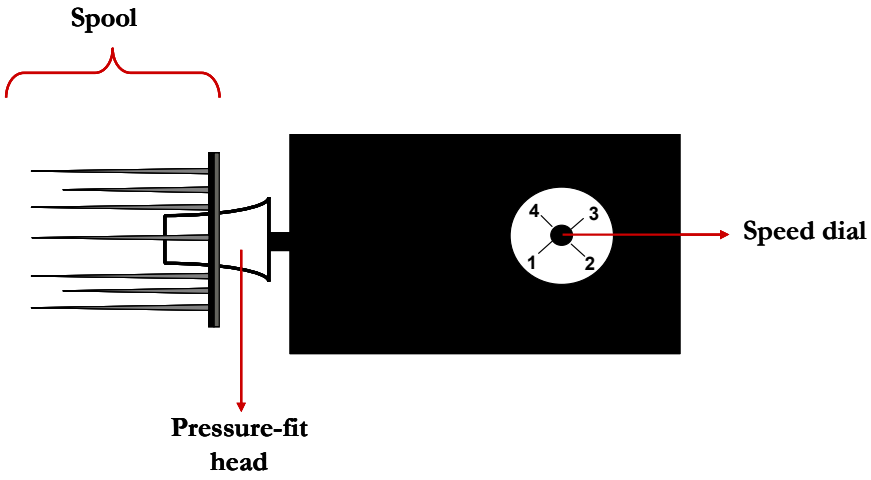

Figure 3.5 Electronic Silk Winder

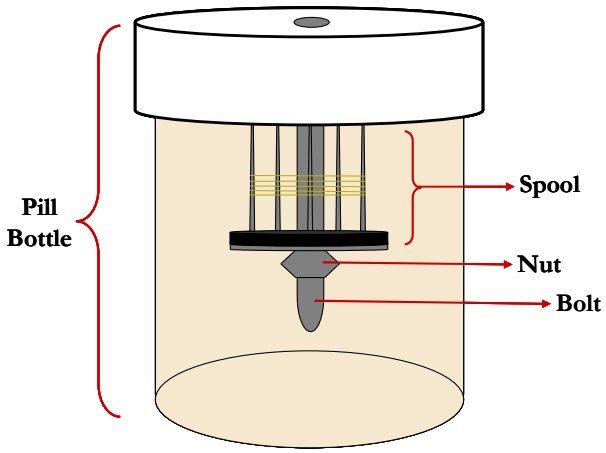

Figure 3.6 Silk Storage Container

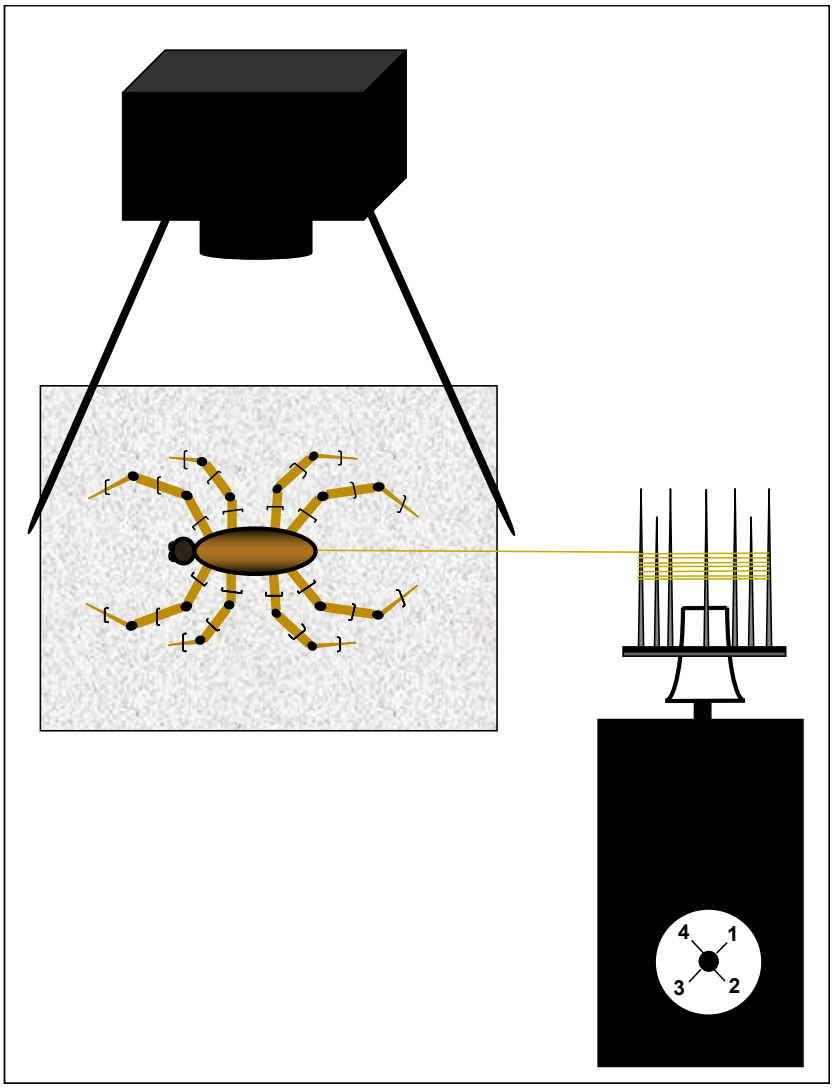

Figure 3.7 Experimental Setup for Thermal Imaging During Silking Process

RESULTS AND DISCUSSION

In order to better understand the spinning process of the spider, a thermal camera was used to detect any possible temperature fluctuations within the spinneret region. The results obtained, although rudimentary, showed an increased temperature in that region when being silked as opposed to pictures taken while the spider was not being silk. The unsilked spider showed the highest temperature region in the upper abdomen, where the cardiac region is located. The thermal images of silked spiders showed two areas of increased temperature (the cardiac region and the spinneret region). The temperatures

observed were between 25°C and 27°C. The thermal images seen in Figures 3.8 to 3.13 were taken using different color scales in order to maximize color contrast. In Figures 3.8, 3.9, 3.11, and 3.12, the color blue corresponded to the highest temperature. In Figures 3.10 and 3.13, the color yellow corresponded to the highest temperature.

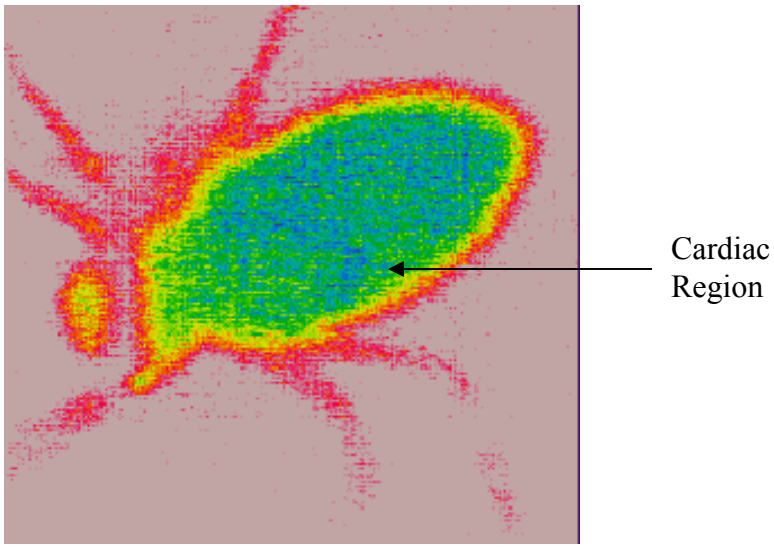

Figure 3.8: Non-Silked Spider: shows increased temperature in cardiac region only

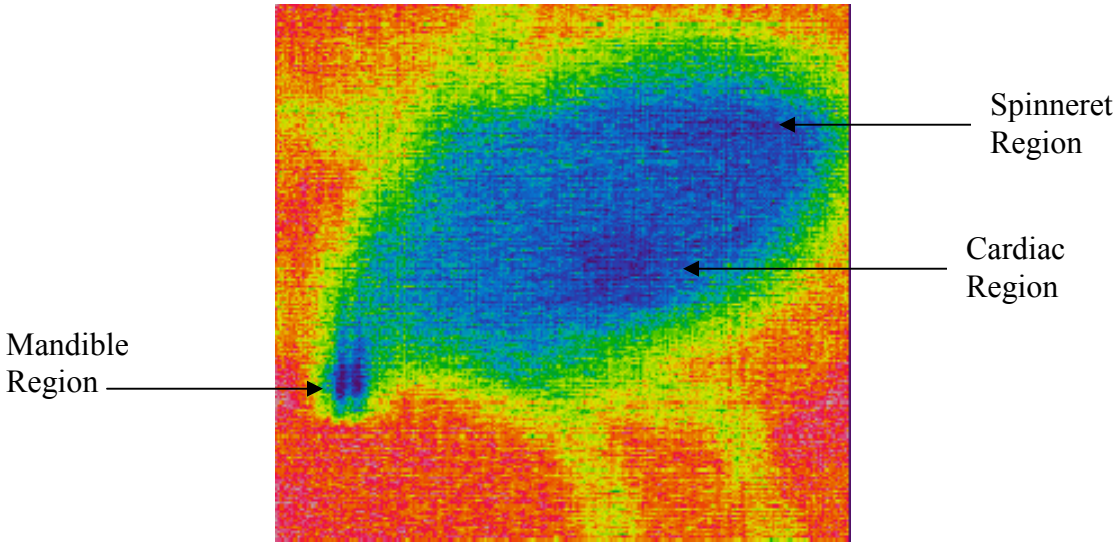

Figure 3.9 Silked Spider 1.a: shows increased temperature in cardiac, spinneret, and mandible regions.

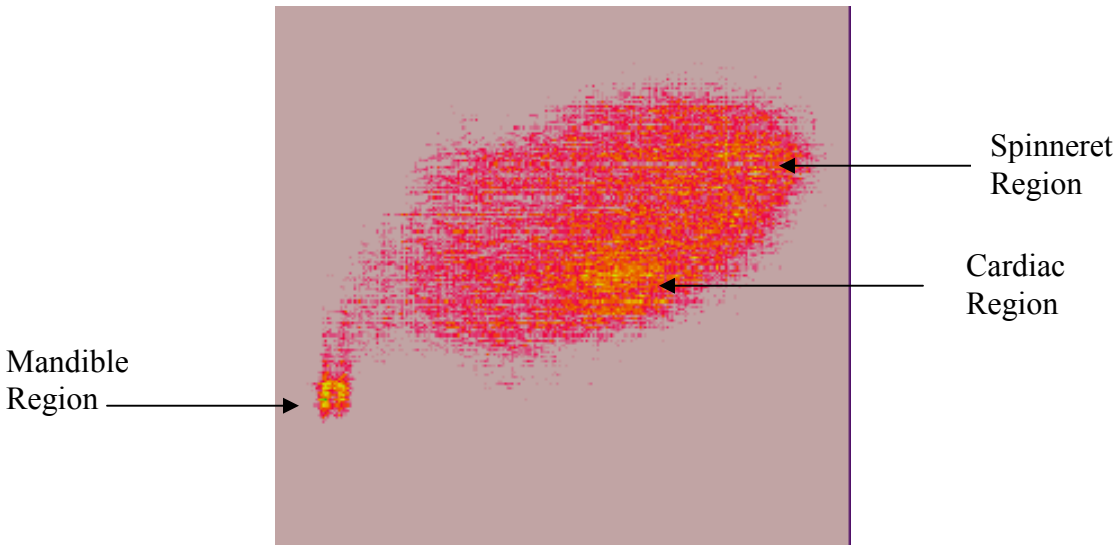

Figure 3.10: Silked Spider 1.b: same image from Figure 3.9 but with inverted color scale

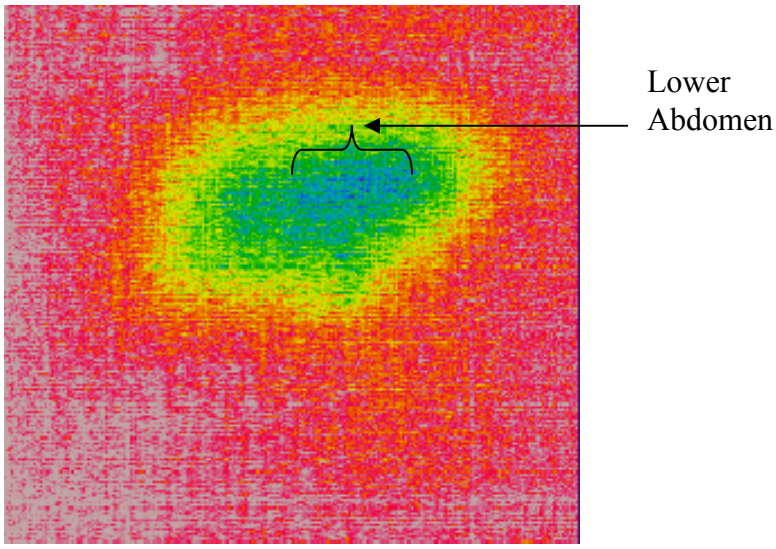

Figure 3.11: Silked Spider 2: shows an oblong, extended increased temperature region in lower abdomen

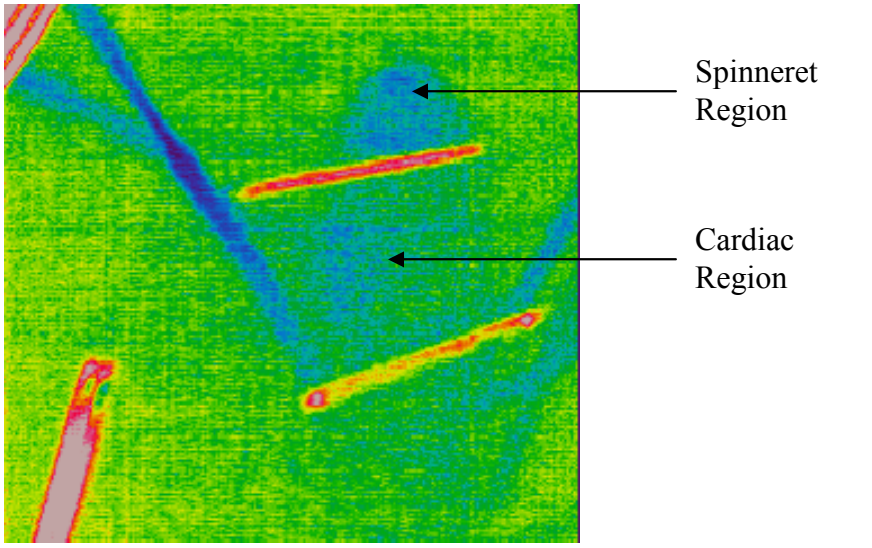

Figure 3.12: Silked Spider 3.a: shows increased temperatures in both spinneret and cardiac regions. (The legs were extended upwards towards the lens, giving them an out-of-scale temperature range)

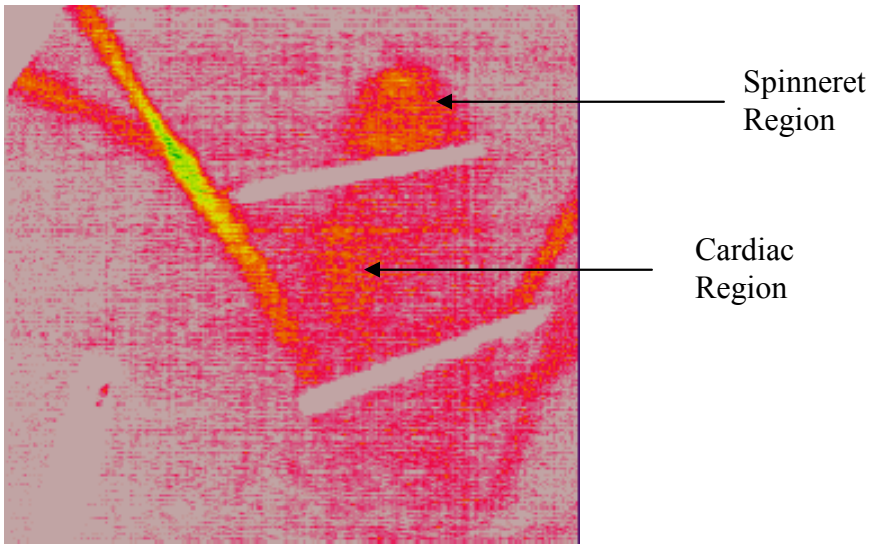

Figure 3.13: Silked Spider 3.b: same image from Figure 3.12 but with inverted color scale

CONCLUSIONS

The images from the thermal camera indicated that an increase in temperature occurred during silking at the spinneret that was of the same order of magnitude as the temperatures observed in the cardiac region. At this level of resolution, it appeared that the temperature increased within the spinneret due to silk production. The cause of the temperature increase is not known nor have the silk been correlated with different

temperature increases. Further work is needed to examine the tensile properties of the silk with the temperature increases to draw any additional conclusions. Also, it needs to be determined if the temperature increase is due to the chemical reactions occurring during silking (an exothermic reaction) or due to the spider redistributing heat to aid the silk production process.

FUTURE WORK

This work examined three main areas of spider silk research necessary for the development of a naturally-based high-performance fiber. First, optimization parameters were explored in order to obtain high cell densities through fermentation. Essential batch media components were outlined that allowed efficient growth of the yeast cultures. Pump profiles were used to maintain exponential growth, enabling high cell densities to be obtained. Further work is needed to optimize the silk production phase which includes: glycerol feeding strategies, methanol feed rates, and pH.

The ultrafiltration concentration method proved useful in concentrating the silk copolymer protein secreted from the cells. However, the high loses in this study need to be quantified and characterized to improve this ultrafiltration step. The column purification of the cell extract resulted in possible formation of silk copolymer protein fibers. The exact cause of the self-assembly conditions are still unknown, and thus work in this area should explore the effects that concentration, pH, temperature, and other parameters have on this protein.

In addition to recombinant silk protein research, continued work with natural spider silk is a key component for understanding the mechanisms for protein self-assembly. The unique spinning method evolved by spiders is a model system for efficiently converting organic substances into highly specialized materials. This thesis established the presence of temperature increases within the spider during the silking process; however, the cause of the temperature increases and the effects the temperature increases have on the silk properties need to be addressed.

APPENDICES

APPENDIX 1
RECIPES

A. YPDS + Zeocin

a. 1% Yeast extract (ACROS)

b. 2% Peptone, from meat (Sigma Cell Culture™)

c. 2% Dextrose, anhydrous (Fisher Scientific)

d. 2% Agar (Sigma Cell Culture™)

e. 1 M D-Sorbitol, 98% (Sigma®)

f. 100 ug/ml Zeocin

B. BMGH

a. 100mM Potassium Phosphate, pH 6.0 [made from Potassium Phosphate, monobasic, HPLC grade (Fisher Scientific) and Potassium Phosphate, dibasic, anhydrous, p.a. (ACROS Organics)}

b. 1.34% Yeast Nitrogen Base without Amino Acids (Difco™)

c. 4×10^{-5} % D-Biotin (Fisher Scientific)

d. 1% Glycerol, 99+% (ACROS)

e. 4×10^{-3}% L-Histidine, monohydro-chloride monohydrate (ICN Biomedicals, Inc.)

f. Deionized water to 1 L

C. Batch Media A (I L)

a. 26.7 ml Phosphoric acid, reagent, ACS, 85+% (ACROS)

b. 0.93 g Calcium Sulfate, anhydrous, 99% (ACROS Organics)

c. 18.2 g Potassium Sulfate, reagent, ACS (ACROS Organics)

d. 14.9 g Magnesium Sulfate, anhydrous (Sigma Cell Culture™)

e. 4.13 g Potassium Hydroxide, reagent, ACS, pellets, 85% (ACROS)

f. 20 g Glycerol, 99+% (ACROS)

g. 0.8 mg D-Biotin (Fisher Scientific)

h. 0.1 g L-Histidine, monohydro-chloride monohydrate (ICN Biomedicals, Inc.)

i. 6 ml Trace metal solution (See Media E)

j. Deionized water to 1 L

D. Batch Media B (1L)

a. 50 mM Potassium phosphate, pH 6.0 [made from Potassium Phosphate, monobasic, HPLC grade (Fisher Scientific) and Potassium Phosphate, dibasic, anhydrous, p.a. (ACROS Organics)}

b. 30 g Glycerol, 99+% (ACROS)

c. 9.9 g Ammonium Sulfate, laboratory grade (Fisher Scientific)

d. 1.9 g Potassium phosphate, monobasic HPLC grade (Fisher Scientific)

e. 1.0 g Magnesium sulfate, anhydrous (Sigma Cell Culture™)

f. 0.2 g Calcium chloride (ICN Biomedicals, Inc.)

g. 0.2 g Sodium chloride, USP/FCC, (Fisher Scientific)

h. 0.1 g L-Histidine, monohydro-chloride monohydrate (ICN Biomedicals, Inc.)

i. 0.8 mg D-Biotin (Fisher Scientific)

j. Deionized water to 1 L

E. Trace Metal Solution (1L)

a. 6.0 g Copper (II) Sulfate, pentahydrate, reagent, ACS, fine crystals (ACROS Organics)
b. 0.08 g Sodium iodide, 99+%, reagent, ACS (Aldrich Chemical Company)
c. 3.0 g Manganese sulfate, anhydrous (Sigma Cell Culture™)
d. 0.2 g Sodium molybdate (VI) dehydrate, 99+% (ACROS Organics)
e. 0.02 g Boric acid, 99+%, powder (ACROS)
f. 0.5 g Cobalt chloride, hexahydrate, minimum 99% (Sigma®)
g. 20.0 g Zinc chloride, reagent, ACS, 97+% (ACROS Organics)
h. 65.0 g Iron (II) sulfate, heptahydrate, p.a. (ACROS Organics)
i. 0.2 g D-Biotin (ACROS)
j. 5.0 ml Sulfuric acid, reagent, ACS (ACROS)
k. Deionized water to 1 L

F. Fed Batch Media (1L)

a. 540 g Glycerol, 99+ (ACROS)
b. 28 g Ammonium sulfate, laboratory grade (Fisher Scientific)
c. 5.4 g Potassium phosphate, monobasic HPLC grade (Fisher Scientific)
d. 2.8 g Magnesium sulfate, anhydrous (Sigma Cell Culture™)
e. 0.6 g Calcium chloride (ICN Biomedicals, Inc.)
f. 0.6 g Sodium chloride, USP/FCC, (Fisher Scientific)
g. 1.8 g L-Histidine, monohydro-chloride monohydrate (ICN Biomedicals, Inc.)
h. 2.0 mg D-Biotin (Fisher Scientific)
i. 12 ml Trace metal solution (See Media E)
j. Deionized water to I L

G. Induction Media (1L)

a. 740 ml 100% Methanol, optima (Fisher Scientific)

b. 12 ml Trace metal solution (See Media E)

c. 1.85 ml L-Histidine, monohydro-chloride monohydrate (ICN Biomedicals, Inc.)

H. 1X Binding Buffer

a. 5 mM Imidazole, 99+% (ACROS Organics)

b. 0.5 M Sodium chloride, USP/FCC, (Fisher Scientific)

c. 20 mM Tris-HCl pH 8.0, ultrapure (Invitrogen)

I. Sample Buffer (2X)

a. 4.0 ml 10% (w/v) Sodium dodecyl sulfate (SDS), electrophoresis grade (BioRad)

b. 2.0 ml Glycerol, 99+ (ACROS)

c. 1.0 ml 0.1% (w/v) Bromophenol blue, sodium salt (J.T. Baker, Inc.)

d. 2.5 ml 0.5 M Tris-HCl, pH 6.8 (MBL International)

e. 2% (v/v) 2-β Mercaptoethanol (J.T. Baker, Inc.)

f. Deionized water to 10 ml

J. Running Buffer (10X)

a. 121 g Tris base, molecular biology grade (Promega)

b. 238 g Hepes (Fisher Scientific)

c. 10 g Sodium dodecyl sulfate (SDS), electrophoresis grade (BioRad)

d. Deionized water to 1 L

K. Transfer Buffer

a. 25 mM Tris base, molecular biology grade (Promega)

b. 192 mM Glycine (BioRad)

c. 20% (v/v) Methanol, optima (Fisher Scientific)

d. Deionized water to 1 L

e. Adjust to pH 8.3 [using Sodium hydroxide (Mallinckrodt Standard®) and Hydrochloric acid, 2N solution (Fisher Scientific)]

L. PBST (1L)

a. 8 g Sodium chloride, USP/FCC, (Fisher Scientific)

b. 0.2 g Potassium chloride (ICN Biomedicals, Inc.)

c. 1.44 g Sodium phosphate, monobasic, USP/FCC (Fisher Scientific)

d. 0.24 g Potassium phosphate, monobasic HPLC grade (Fisher Scientific)

e. 2 ml Tween® 20 (polyoxyethylene sorbitan monolaurate) (Fisher Scientific)

f. Deionized water to 1 L

g. Adjust pH to 7.2 [using Sodium hydroxide (Mallinckrodt Standard®) and Hydrochloric acid, 2N solution (Fisher Scientific)]

M. 5% Blocking Buffer

a. 33.25 g Powdered Blocker (Nestle® Carnation Instant Nonfat Dry Milk)

b. 665 ml PBST (See Media L)

N. BMMH

a. 100mM Potassium Phosphate, pH 6.0 [made from Potassium Phosphate, monobasic, HPLC grade (Fisher Scientific) and Potassium Phosphate, dibasic, anhydrous, p.a. (Acros Organics)}
b. 1.34% Yeast Nitrogen Base without Amino Acids (Difco™)
c. 4×10^{-5} % D-Biotin (Fisher Scientific)
d. 1% Methanol, optima (Fisher Scientific)
e. 4×10^{-3}% L-Histidine, monohydro-chloride monohydrate (ICN Biomedicals, Inc.)
f. Deionized water to 1 L

O. Breaking Buffer

a. 50 mM Sodium phosphate, pH 7.4, monobasic, USP/FCC (Fisher Scientific)
b. 1 mM PMSF(phenylmethylsulfonyl fluoride) (Research Organics Inc.)
c. 1 mM EDTA (ethylediaminetetraacetic acid), reagent, ACS (ACROS)
d. 5% Glycerol, 99+% (ACROS)

P. Wash I

a. 10 mM Imidazole, 99+% (ACROS Organics)
b. 0.5 M Sodium chloride, USP/FCC (Fisher Scientific)
c. 20 mM Tris HCl pH 8.0, ultrapure (Invitrogen)

Q. Wash II

a. 20 mM Imidazole, 99+% (ACROS Organics)
b. 0.5 M Sodium chloride, USP/FCC (Fisher Scientific)
c. 20 mM Tris HCl pH 8.0, ultrapure (Invitrogen)

R. Elution I

a. 80 mM Imidazole, 99+% (ACROS Organics)

b. 0.5 M Sodium chloride, USP/FCC (Fisher Scientific)

c. 20 mM Tris HCl pH 8.0, ultrapure (Invitrogen)

S. Elution II

a. 150 mM Imidazole, 99+% (ACROS Organics)

b. 0.5 M Sodium chloride, USP/FCC (Fisher Scientific)

c. 20 mM Tris HCl pH 8.0, ultrapure (Invitrogen)

APPENDIX 2

FERMENTATION HISTORY PLOTS

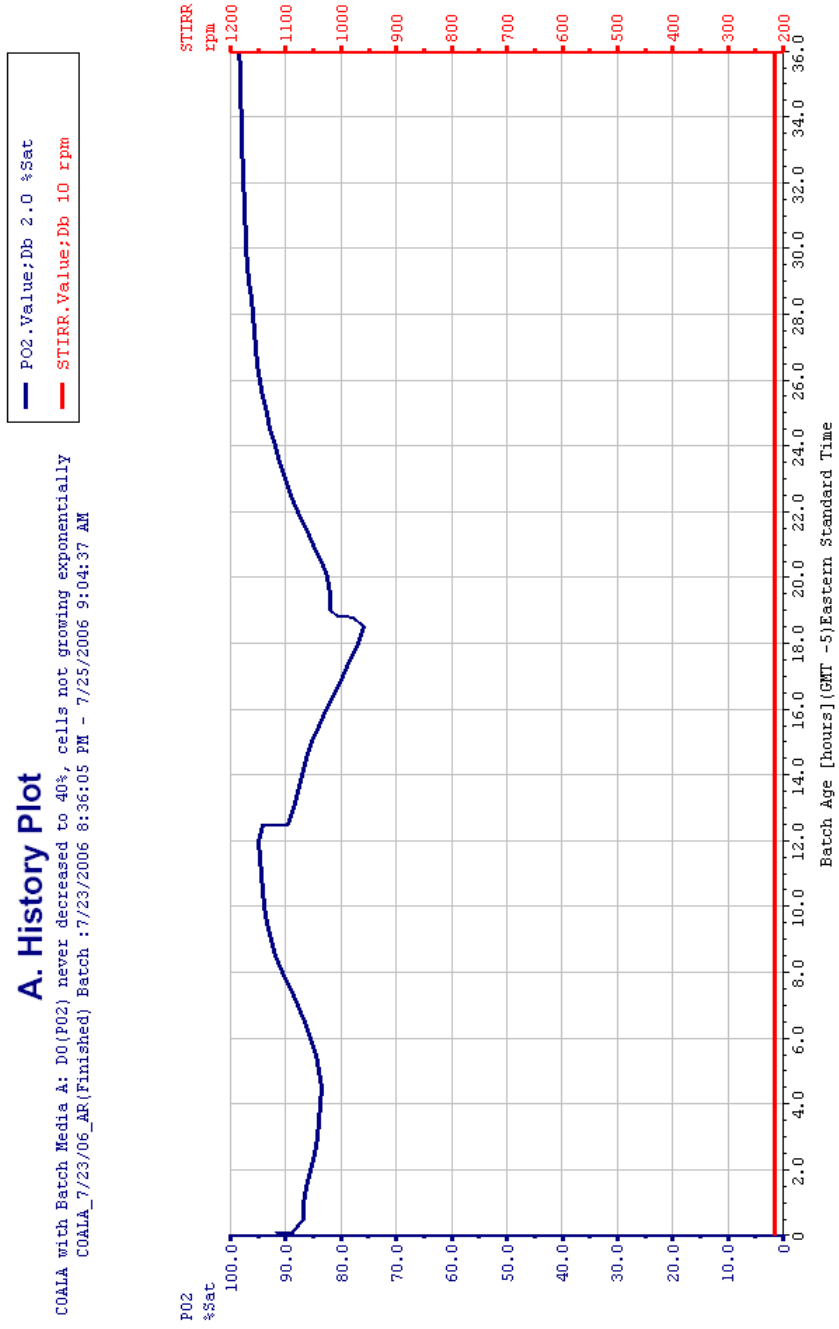

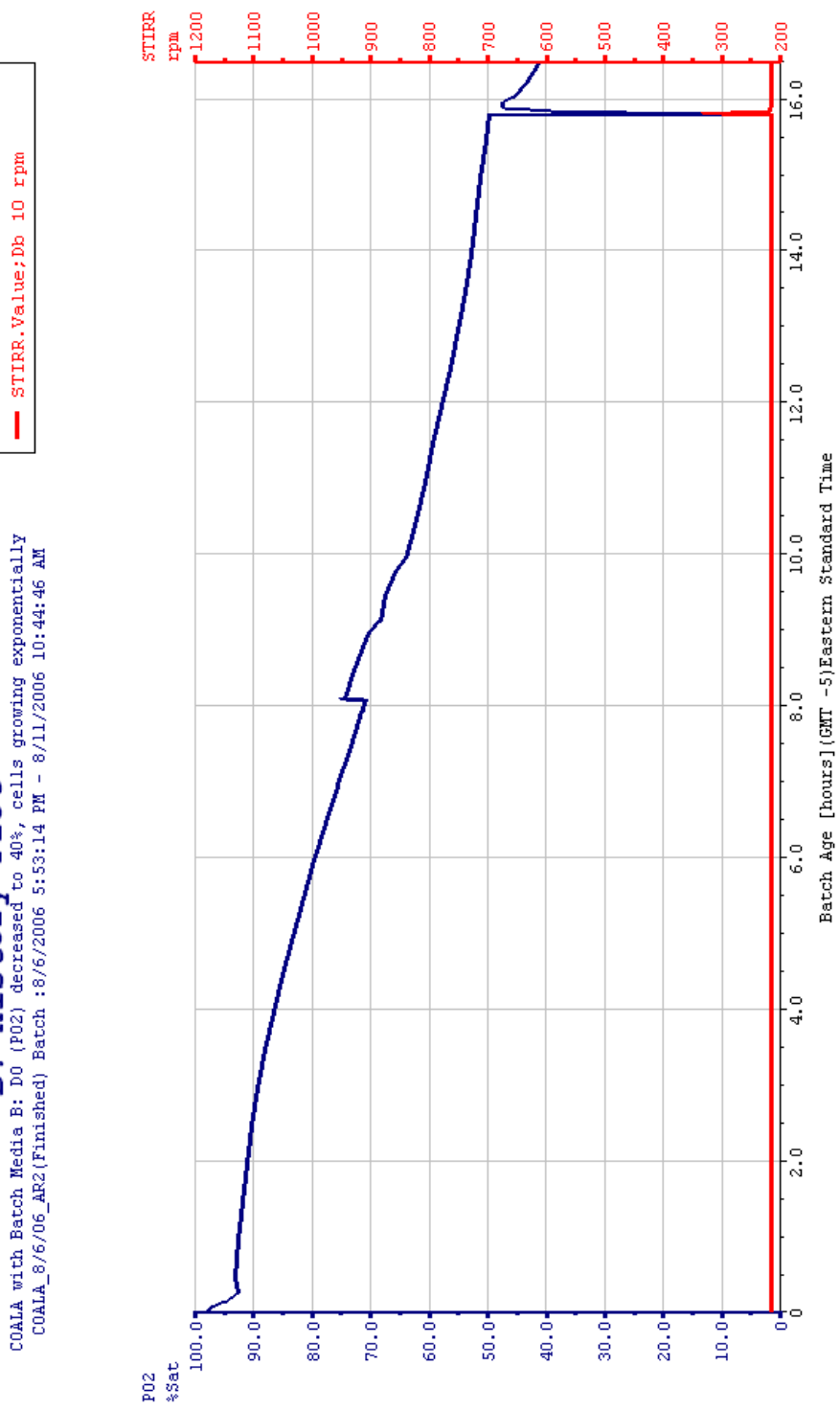
B. History Plot
COA1A with Batch Media B: DO (PO2) decreased to 40%, cells growing exponentially
COA1A_8/6/06_AR2(Finished) Batch :8/6/2006 5:53:14 PM - 8/11/2006 10:44:46 AM
PO2.Value;Db 2.0 %Sat
STIRR.Value;Db 10 rpm
PO2
%Sat
STIRR
rpm
Batch Age [hours](GMT -5)Eastern Standard Time

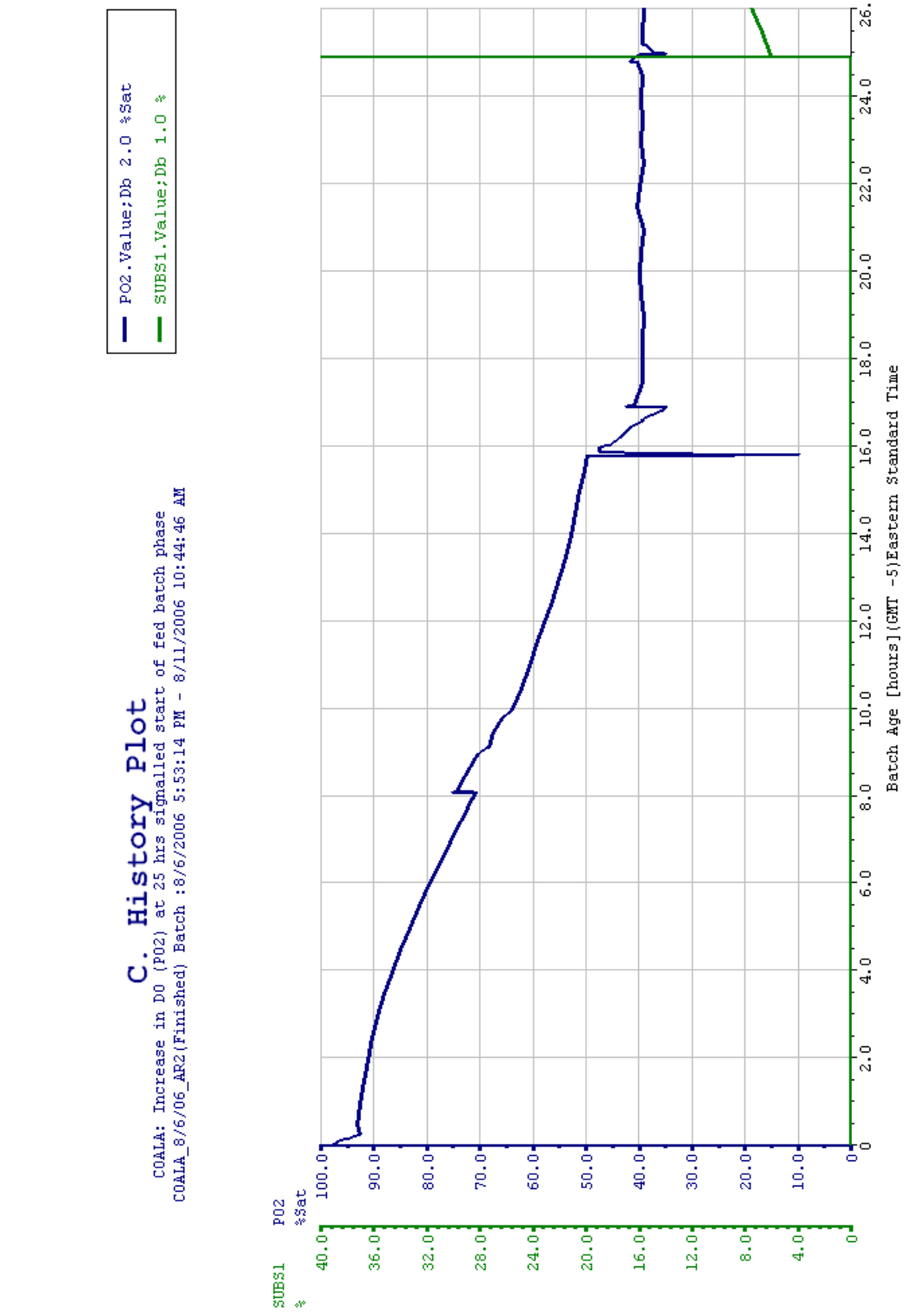
C. History Plot
COALA: Increase in DO (PO2) at 25 hrs signalled start of fed batch phase
COALA_8/6/06_AR2(Finished) Batch :8/6/2006 5:53:14 PM - 8/11/2006 10:44:46 AM
PO2.Value;Db 2.0 %Sat
SUBS1.Value;Db 1.0 %
SUBS1 %
PO2 %Sat
Batch Age [hours](GMT -5)Eastern Standard Time

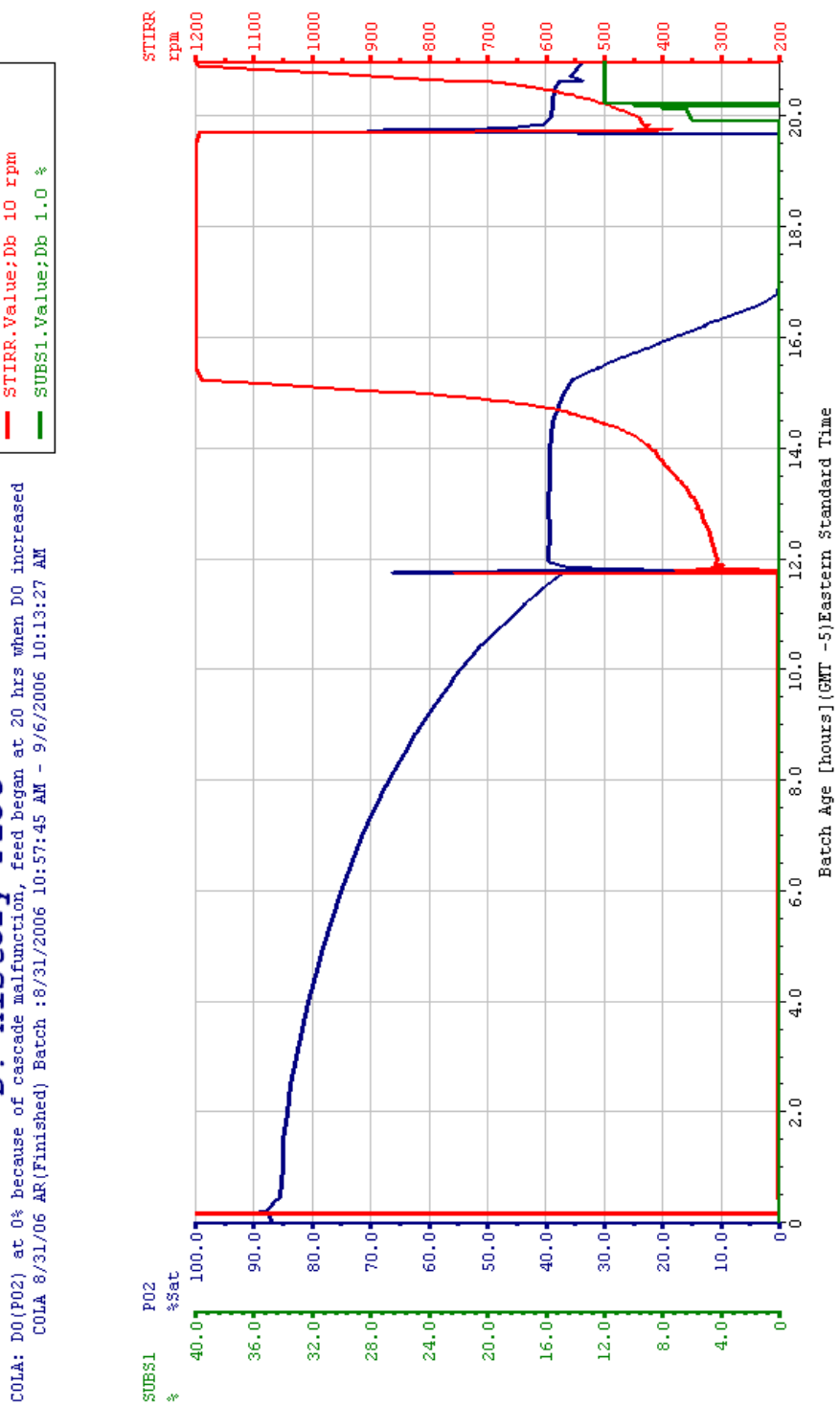
D. History Plot
COLA: DO(PO2) at 0% because of cascade malfunction, feed began at 20 hrs when DO increased
COLA 8/31/06 AR(Finished) Batch :8/31/2006 10:57:45 AM - 9/6/2006 10:13:27 AM
PO2.Value;Db 2.0 %Sat
STIRR.Value;Db 10 rpm
SUBS1.Value;Db 1.0 %
STIRR rpm
SUBS1 %
PO2 %Sat
Batch Age [hours](GMT -5)Eastern Standard Time

E. History Plot

COALA: Feed profile produced linear increase in stir rate

COALA_8/6/06_AR2(Finished) Batch :8/6/2006 5:53:14 PM - 8/11/2006 10:44:46 AM

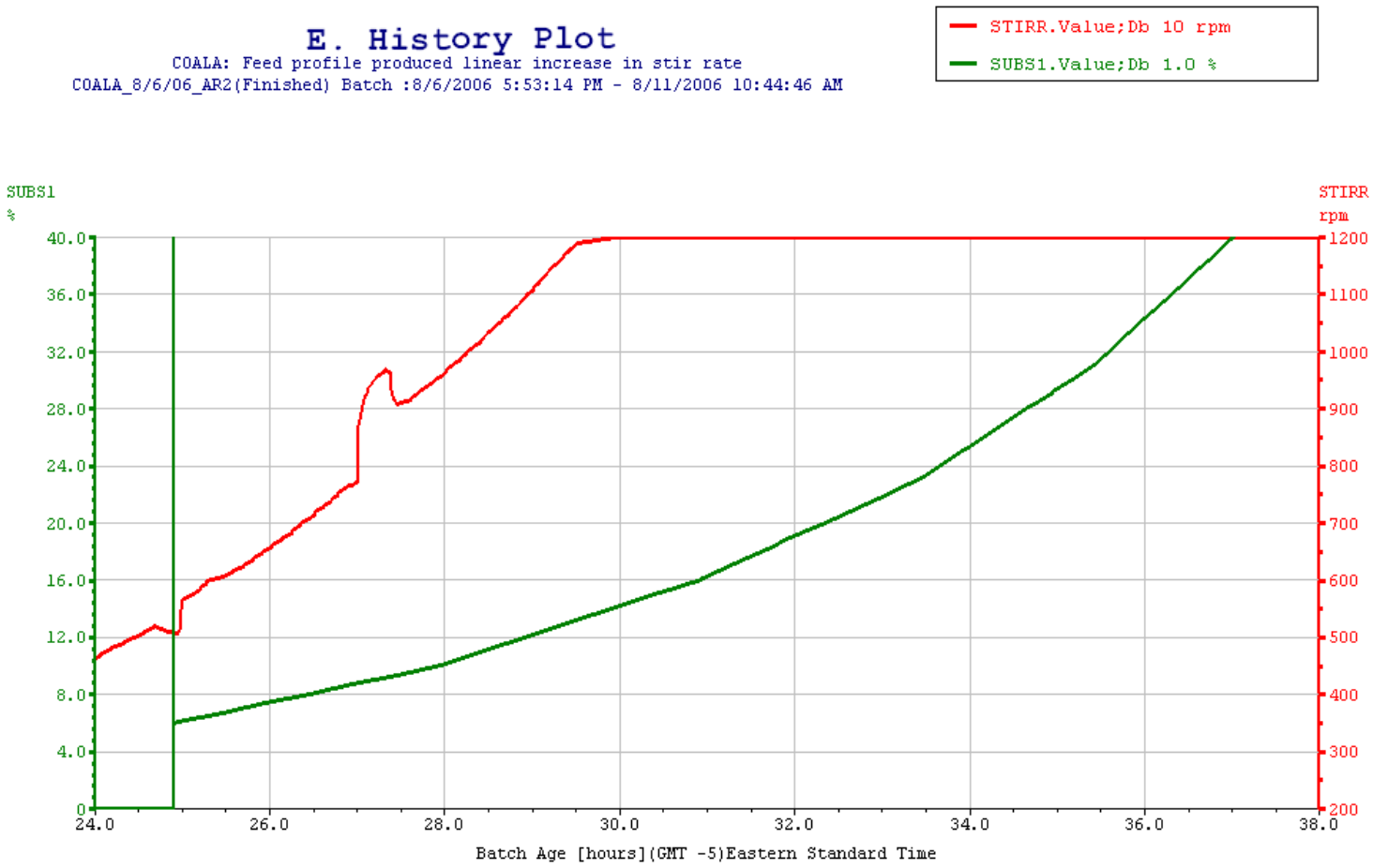

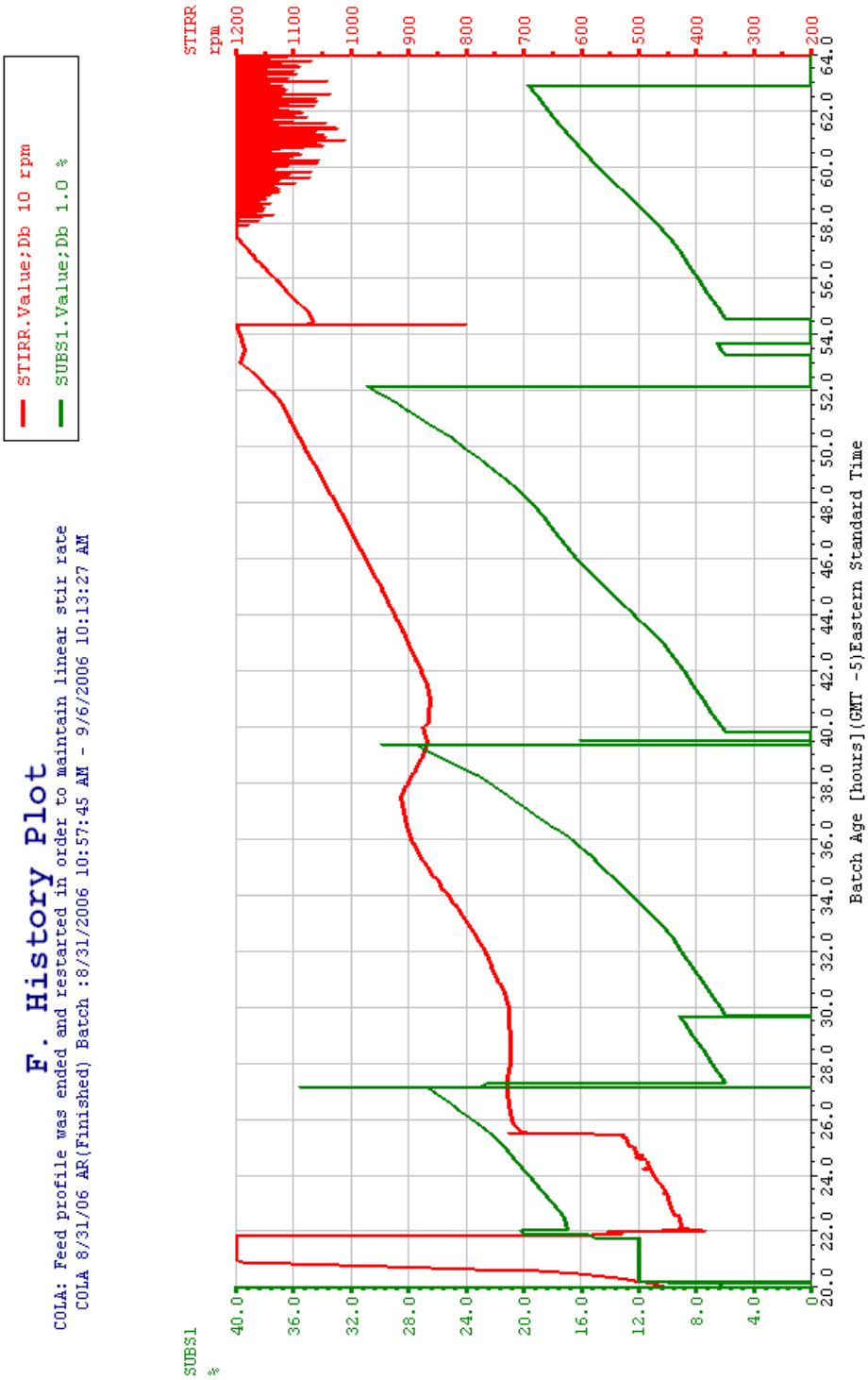
F. History Plot
COLA: Feed profile was ended and restarted in order to maintain linear stir rate
COLA 8/31/06 AR(Finished) Batch :8/31/2006 10:57:45 AM - 9/6/2006 10:13:27 AM
STIRR.Value;Db 10 rpm
SUBS1.Value;Db 1.0 %
STIRR
rpm
SUBS1
%
Batch Age [hours](GMT -5)Eastern Standard Time

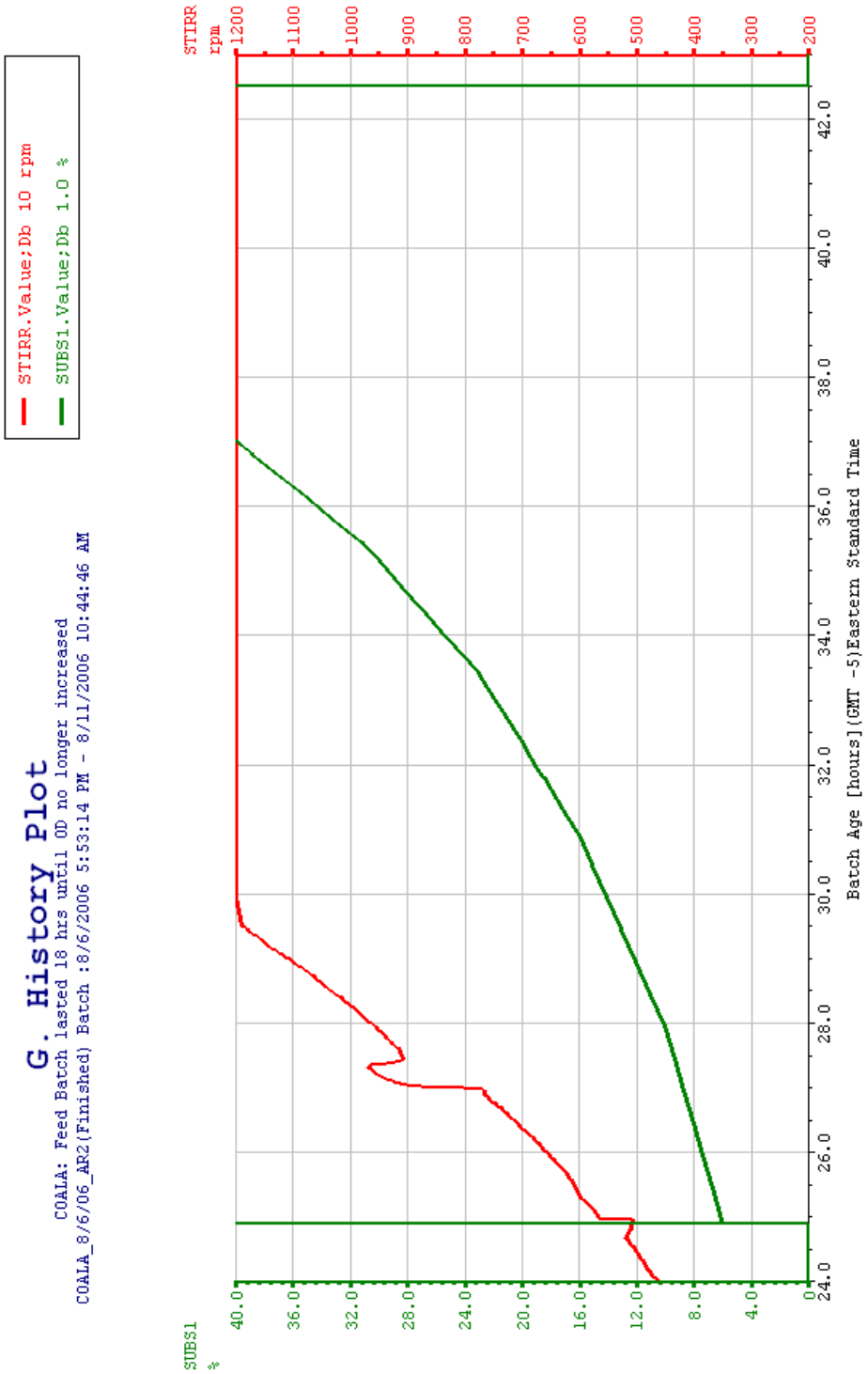
G. History Plot
COALA: Feed Batch lasted 18 hrs until OD no longer increased
COALA_8/6/06_AR2(Finished) Batch :8/6/2006 5:53:14 PM - 8/11/2006 10:44:46 AM
STIRR.Value;Db 10 rpm
SUBS1.Value;Db 1.0 %
STIRR
rpm
SUBS1
%
Batch Age [hours](GMT -5)Eastern Standard Time

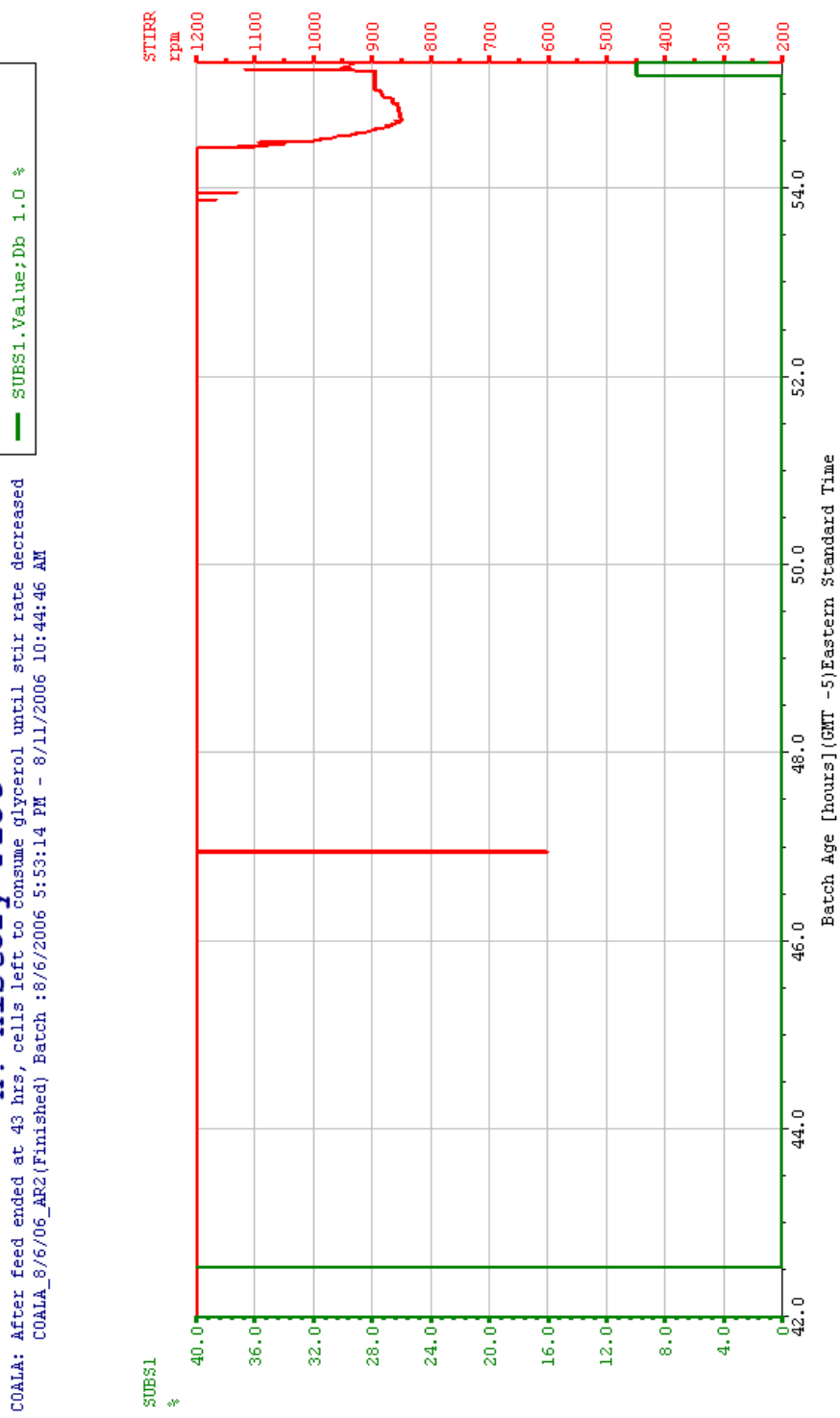
H. History Plot
COALA: After feed ended at 43 hrs, cells left to consume glycerol until stir rate decreased
COALA_8/6/06_AR2(Finished) Batch :8/6/2006 5:53:14 PM - 8/11/2006 10:44:46 AM
STIRR.Value;Db 10 rpm
SUBS1.Value;Db 1.0 %
STIRR
rpm
SUBS1
%
Batch Age [hours](GMT -5)Eastern Standard Time

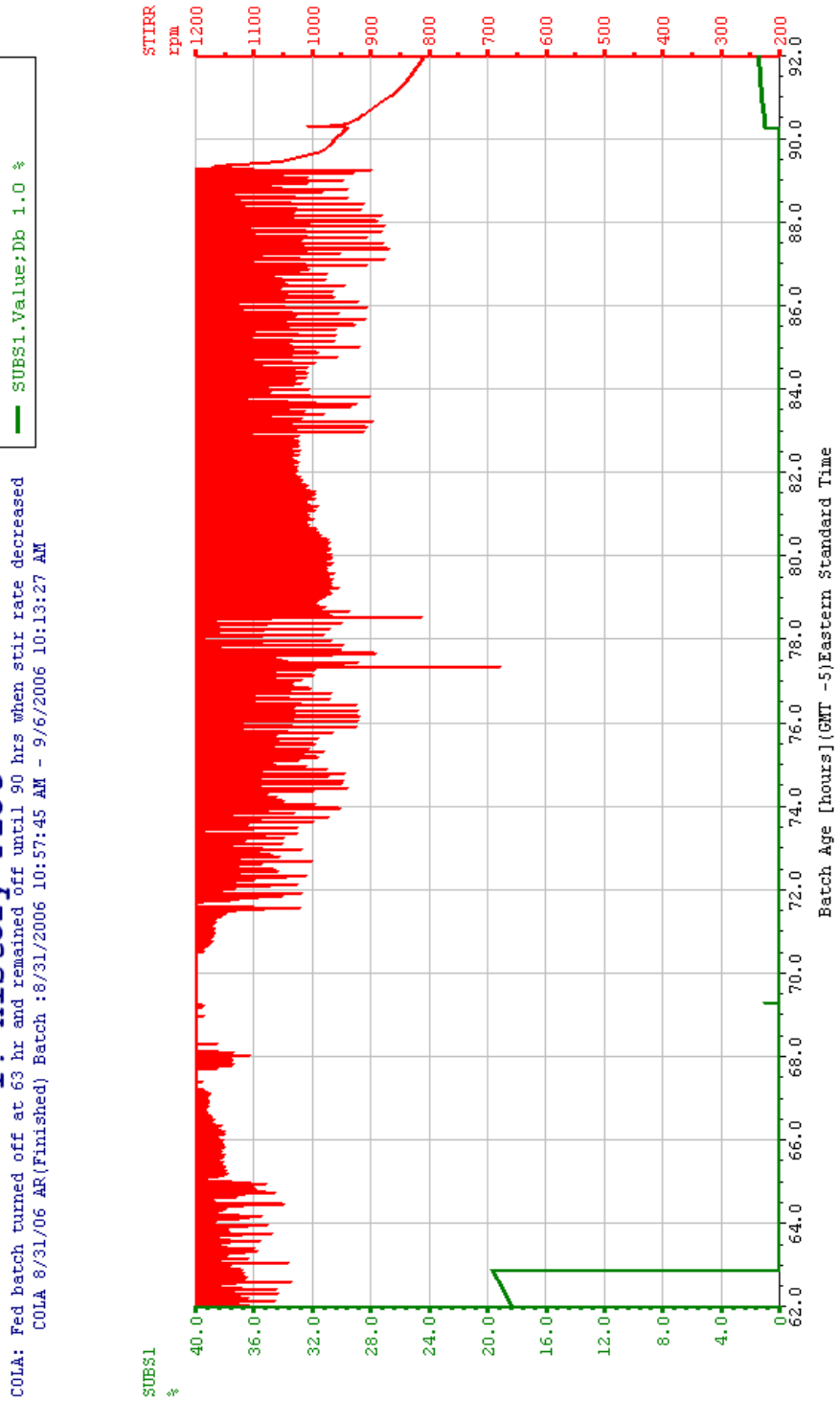
I. History Plot
COLA: Fed batch turned off at 63 hr and remained off until 90 hrs when stir rate decreased
COLA 8/31/06 AR(Finished) Batch :8/31/2006 10:57:45 AM - 9/6/2006 10:13:27 AM
STIRR.Value;Db 10 rpm
SUBS1.Value;Db 1.0 %
STIRR
rpm
SUBS1
%
Batch Age [hours](GMT -5)Eastern Standard Time

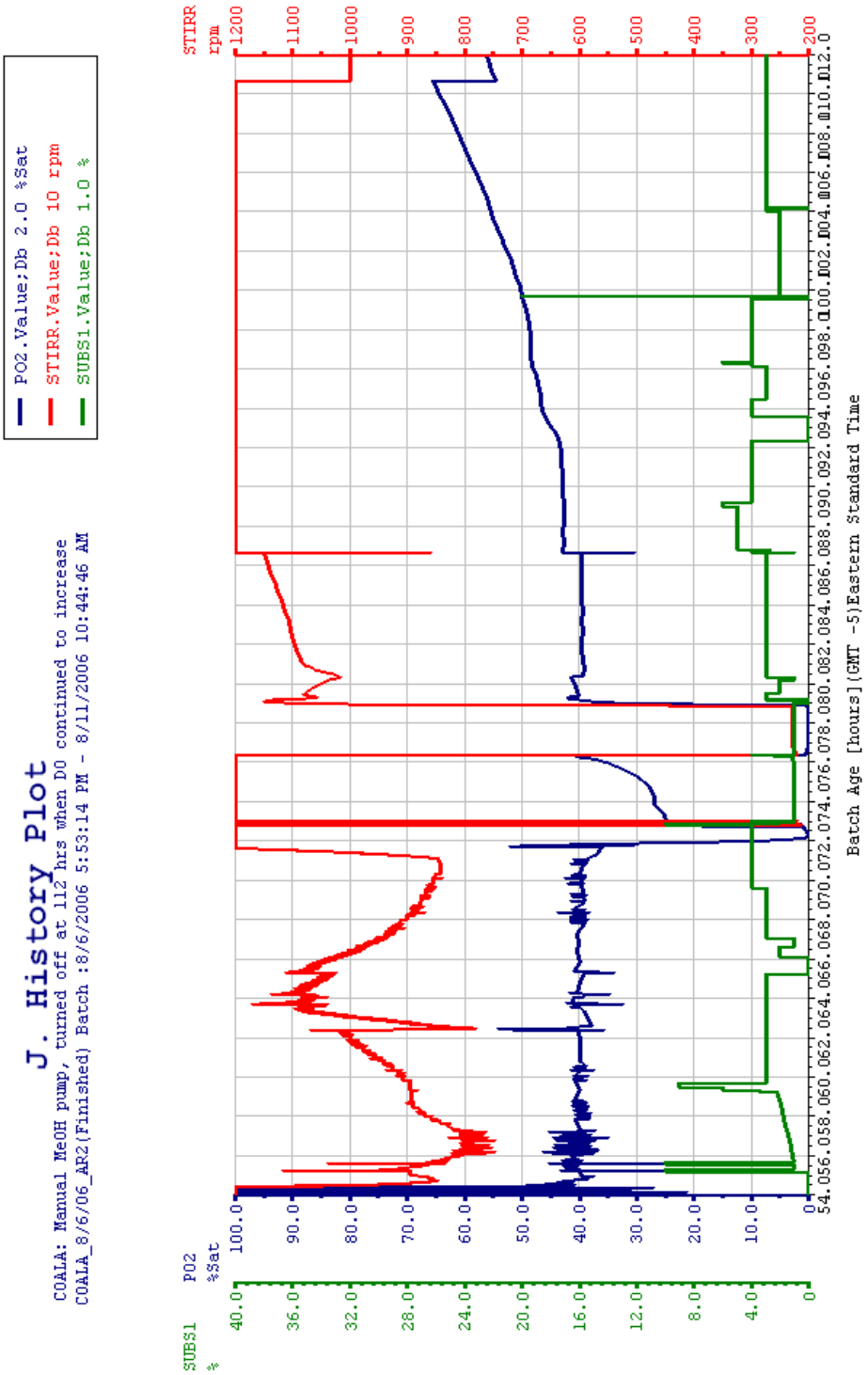
J. History Plot
COALA: Manual MeOH pump, turned off at 112 hrs when DO continued to increase
COALA_8/6/06_AR2(Finished) Batch :8/6/2006 5:53:14 PM - 8/11/2006 10:44:46 AM
PO2.Value;Db 2.0 %Sat
STIRR.Value;Db 10 rpm
SUBS1.Value;Db 1.0 %
SUBS1 %
PO2 %Sat
STIRR rpm
Batch Age [hours](GMT -5)Eastern Standard Time

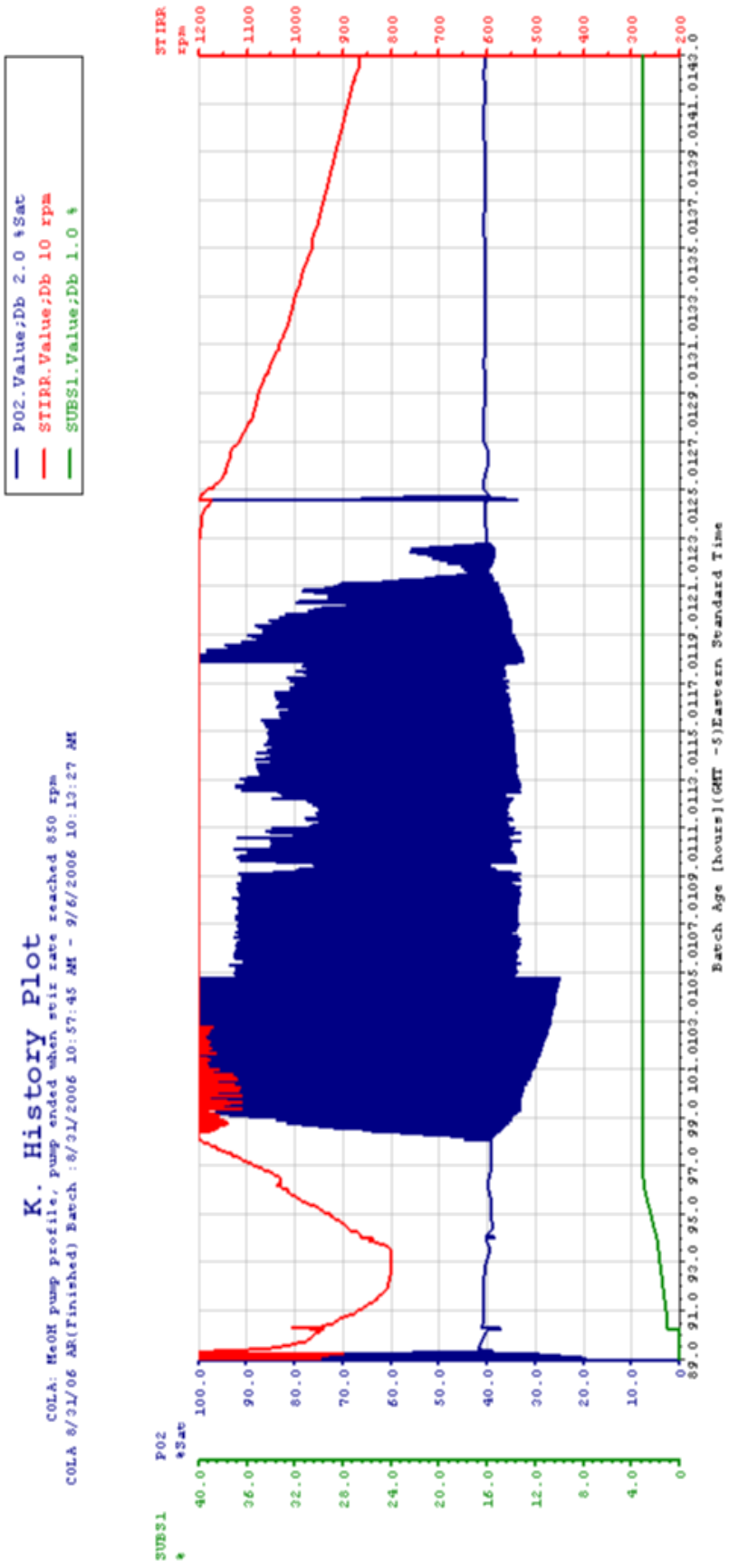
K. History Plot
COLA: MeOH pump profile, pump ended when stir rate reached 850 rpm
COLA 8/31/06 AR(Finished) Batch :8/31/2006 10:57:45 AM - 9/6/2006 10:13:27 AM
P02.Value;Db 2.0 %Sat
STIRR.Value;Db 10 rpm
SUBS1.Value;Db 1.0 %
STIRR rpm
P02 %Sat
SUBS1 %
Batch Age [hours](GMT -5)Eastern Standard Time

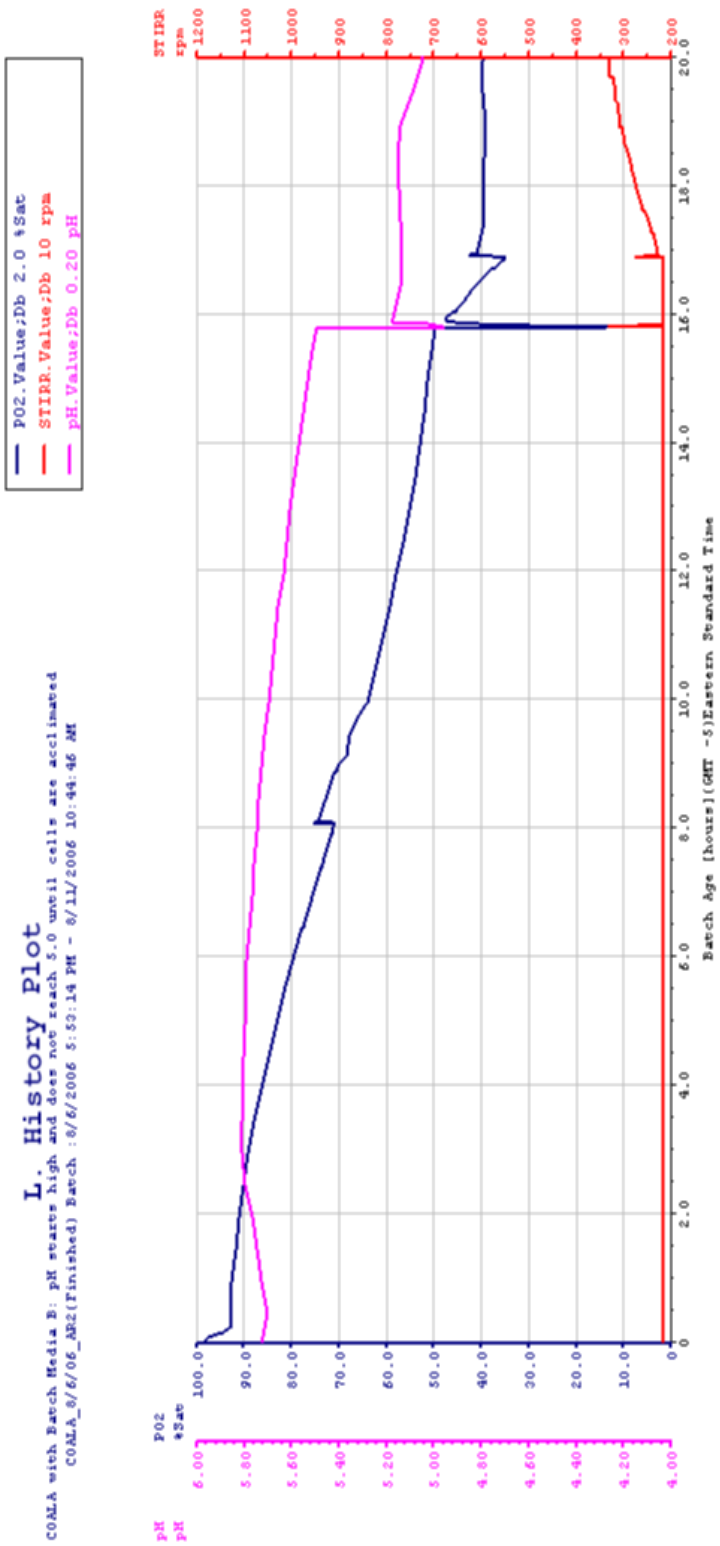
L. History Plot
COALA with Batch Media B: pH starts high and does not reach 5.0 until cells are acclimated
COALA_8/6/06_AB2(Finished) Batch : 8/6/2006 5:53:14 PM - 8/11/2006 10:44:46 AM
P02.Value;Db 2.0 %Sat
STIRR.Value;Db 10 rpm
pH.Value;Db 0.20 pH
STIRR rpm
P02 %Sat
pH pH
Batch Age [hours](GMT -5)Eastern Standard Time

APPENDIX 3

SPIDER PICTURES

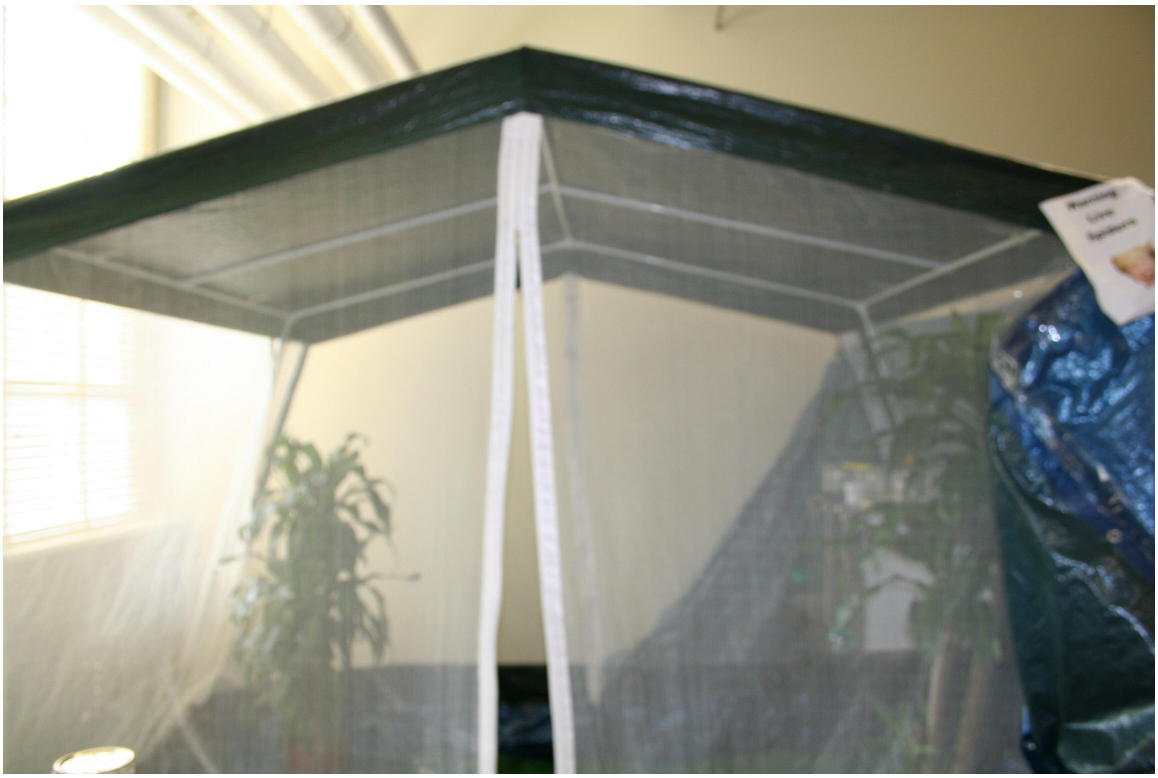

A Spider Tent

B. Spider Climbing Out of Jar onto String

C. Spider Capturing Cricket

D. Spider Captured in Jar Before Being Placed in Refrigerator

E. Spider Pinned onto Styrofoam for Silking

F. Measurements Taken Prior to Silking

LITERATURE CITED

P. pastoris Fermentation using a BioFlo 110 Benchtop Fermentor, vol. 2006: New Brunswick Scientific.

Amersham. (2001). Protein Purification Handbook, vol. 2006: Amersham Biosciences.

Anspach, F. B., Curbelo, D., Hartmann, R., Garke, G. and Deckwer, W. D. (1999). Expanded-bed chromatography in primary protein purification. *J Chromatogr A* **865**, 129-44.

Azuma, A. (February 28, 2006). The Biokinetics of Flying and Swimming: American Instituteof Aeronautics and Astronautics.

Bailey, S. M., Meagher, M.M. (2000). Separation of Soluble Protein from Inclusion Bodies in *Escherichia coli* Lysate Using Crossflow Microfiltration. *J. Membr. Sci.* **166**, 137-146.

Bar-Cohen, Y., Cynthia L. Breazeal. (May 13, 2003). Biologically Inspired Intelligent Robots: The International Society for Optical Engineering.

Belter, P. A., C.L. Cussler, and W.S. Hu. (1988). Bioseparations. New York: John Wiley and Sons.

Benyus, J. M. (May 1998). Biomimicry: Innovation Inspired by Nature: William Morrow and Co.

Blattner, F. R., Plunkett, G., 3rd, Bloch, C. A., Perna, N. T., Burland, V., Riley, M., Collado-Vides, J., Glasner, J. D., Rode, C. K., Mayhew, G. F. et al. (1997). The complete genome sequence of Escherichia coli K-12. *Science* **277**, 1453-74.

Breirley, R. A., Bussineau, C., Kosson, R., Melton, A., Siegel, R. S. (1990). Fermentation Development of Recombinant *Pichia pastoris* Expressing the Recombinant Gene: Bovine Lysozyme. *Ann. New York Acad. Sci.* **589**, 350-362.

Chang, Y. K. a. C., H.A. (1996). Development of Operating Conditions for Protein Purification Using Expanded Bed Techniques: The Effect of the Degree of Bed Expansion on Adsoprtion Performance. *Biotech. Bioeng.* **49**, 512-526.

Charoenrat, T. (2005). Process Design for Production of Thai Rosewood B-glucosidase in *Pichia pastoris*. In *School of Biotechnology*, pp. 50. Stockholm: Royal Institute of Technology.

Chaudhuri, T., Horii K, Yoda T, Arai M, Nagata S, Terada TP, Urchiyama H, Ikura T, Tsumoto K, Kataoka H, Matsushima M, Kuwajima K, Kumagai I. (1999). Effects of the extra N-terminal Methionine Residue on the Stability and Folding of Recombinant Alpha-lactalbumin expressed in Escherichia coli. *J. Mol. Biol.* **285**, 1179-1194.

Cheryan, M. (1998). Ultrafiltration and Microfiltration Handbook. Lancaster, PA: Technomic Publishing.

Chiruvolu, V., C. J., Meagher MM. (1997). Recombinant protein production in an alcohol oxidase-defective strain of *Pichia pastoris* in fedbtach fermentations. *Enzyme Microb Technol.* **21**, 277-283.

Cino, J. (1999). High-Yield Protein Production from *Pichia pastoris* Yeast: A Protocol for Benchtop Fermentation. *American Biotechnology Laboratory* **17**, 10-12.

Cohen, B. *Pichia* Protein Expression System, vol. 2006: Research Corporation Technologies.

Cohen, S. N., Annie C. Y. Chang, Herbert W. Boyer, and Robert B. Helling. (1973). Construction of Biologically Functional Bacterial Plasmids In Vitro *PNAS* **70**, 3240-3244.

Cos, O., Ramon, R., Montesinos, J. L. and Valero, F. (2006). Operational strategies, monitoring and control of heterologous protein production in the methylotrophic yeast Pichia pastoris under different promoters: A review. *Microb Cell Fact* **5**, 17.

Cregg, J. M., Vedvick, T. S. and Raschke, W. C. (1993). Recent advances in the expression of foreign genes in Pichia pastoris. *Biotechnology (N Y)* **11**, 905-10.

Curbelo, D., G. Garke, R.C. Guilarete, F.B. Anspach, and W.D. Deckwer. (2003). Cost Comparison of Protein Capture from Cultivation Broths by Expanded and Pack Bed Adsoption *Eng. Life. Sci.* **3**, 406-415.

Daly, R. and Hearn, M. T. (2005). Expression of heterologous proteins in Pichia pastoris: a useful experimental tool in protein engineering and production. *J Mol Recognit* **18**, 119-38.

Drabble, E. and Scott, D. G. (1907). On the Effect of Acids, Alkalis, and Neutral Salts on the Fermentative Activity and on the Rate of Multiplication of Yeast Cells. *Biochem J* **2**, 340-9.

Elices, M., Perez-Riguerio, J., Plaza, G., and G. Guinea. (2005). Finding Inspiration in *Argiope trifasciata* spider silk fibers. *JOM,* February.

Evan, G. I., Lewis, G. K., Ramsay, G., and Bishop, V.M. (1985). Isolation of Monoclonal Antibodies Specific for *c-myc* Proto-oncogene Product. *Mol. Cell. Biol.* **5**, 3610-3616.

Faber, e. a. (1995). Review: Methylotrophic Yeast as Factories for the Production of Foreign Protein. *Yeast* **11**, 1331-1344

Feldman, H. (2005). Yeast Molecular Biology: A Short Compendium on Basic Features and Novel Aspects, vol. 2006: Adolf-Butenandt- Institute.

Foelix, R. (1996). Biology of Spiders. Oxford, UK: Oxford University Press.

Forbes, P. (August 15, 2005). The Gecko's Foot: Fourth Estate.

Gasch, A. P., Margaret Werner-Washburne. (2002). The genomics of yeast responses to environmental stress and starvation. *Functional and Integrative Genomics* **4**, 181-192.

Gellissen, G., Melber, K., Janowicz, Z. A., Dahlems, U. M., Weydemann, U., Piontek, M., Strasser, A. W. and Hollenberg, C. P. (1992). Heterologous protein production in yeast. *Antonie Van Leeuwenhoek* **62**, 79-93.

Ghosh, R. (2003). Protein Bioseparation: An Overview. In *Protein Bioseparation Using Ultrafiltration: Theory, Applications, and New Developments*. Danvers, MA: Imperial College Press.

Gleeson, M. a. S. P. (1988). The Methylotrophic Yeasts. *Yeast* **4**, 1-15.

Gosline, J. M., Guerette, P. A., Ortlepp, C. S. and Savage, K. N. (1999). The mechanical design of spider silks: from fibroin sequence to mechanical function. *J Exp Biol* **202**, 3295-303.

Hayashi, C. Y., Shipley, N. H., Lewis, R. V. (1999). Hypotheses that correlate the sequence, structure, and mechanical properties of spider silk proteins. *Int. J. Biol. Macromolecules* **24**.

Hengen, P. (1995). Purification of His-Tag fusion proteins from Escherichia coli. *Trends Biochem Sci* **20**, 285-6.

Hinman, M. B., and Lewis, R.V. (1992). of a clone encoding a second dragline silk fibroin. *J. Biol. Chem.* **267**, 19320-19324

Hochuli, E. (1988). Large-scale chromatography of recombinant proteins. *J Chromatogr* **444**, 293-302.

Hyde, N. (1984). The Queen of Textiles. *National Geographic* **165**, 3-49.

Hyjorth, R. (1997). Expanded Bed Adsorption in Industrial Bioprocessing: Recent Developments. *Tibtech.* **15**, 230-235.

Inan, M. and Meagher, M. M. (2001). The effect of ethanol and acetate on protein expression in Pichia pastoris. *J Biosci Bioeng* **92**, 337-41.

Invitrogen. (2001). The *Pichia pastoris* Expression System, vol. 2006: Research Corporation Technologies.

Itakura, K., Hirose, T., Crea, R., Riggs, A. D., Heyneker, H. L., Bolivar, F. and Boyer, H. W. (1977). Expression in Escherichia coli of a chemically synthesized gene for the hormone somatostatin. *Science* **198**, 1056-63.

Lee, J. a. K. K. (1980). Taxonomic Study of Methanol-Assimilating Yeasts. *J. Appl. Microbiol.* **26**, 113-158.

Lee, P. S. and Lee, K. H. (2003). Escherichia coli--a model system that benefits from and contributes to the evolution of proteomics. *Biotechnol Bioeng* **84**, 801-14.

Lewis, R. V., Hinman, M., Kothakota, S. and Fournier, M. J. (1996). Expression and purification of a spider silk protein: a new strategy for producing repetitive proteins. *Protein Expr Purif* **7**, 400-6.

Lo, Y. M., Yang S.T., Min, D.B. (1996). Kinetic and Feasability Studies of Ultrafiltration of Viscous Xantham Gum Fermentation Broth: Process and Economic Analyses. *J. Food Eng.* **31**, 219-236.

Lucas, F. (1964). *Discovery* **25**, 20.

Lueking, A., Holz, C., Gotthold, C., Lehrach, H. and Cahill, D. (2000). A system for dual protein expression in Pichia pastoris and Escherichia coli. *Protein Expr Purif* **20**, 372-8.

Marston, F. A. (1986). The purification of eukaryotic polypeptides synthesized in Escherichia coli. *Biochem J* **240**, 1-12.

Mayson, B. E., Kilburn, D. G., and Zamost, B. L. . (2003). Effects of Methanol Concentration on Expression Levels of Recombinant Protein in Fed-Batch Cultures of *Pichia pastoris*. *Biotech. Bioeng.* **81**, 291-298.

Monsalve, R. I., Lu, G. and King, T. P. (1999). Expressions of recombinant venom allergen, antigen 5 of yellowjacket (Vespula vulgaris) and paper wasp (Polistes annularis), in bacteria or yeast. *Protein Expr Purif* **16**, 410-6.

Ohashi, R., Mochizuki E, Suzuki T. (1999). A Mini-Scale Mass Production and Separation System for Secretory Heterologous Proteins by Perfusion Culture of Recombinant Pichia Pastoris using a Shaken Ceramic Membrane Flask. *Biosci. Bioeng.* **87**, 655-660.

Pan, Z. J., C. P. Li, and Q. Xu (2004). Active control on molecular conformations and tensile properties of spider silk. *Journal of Applied Polymer Science* **92**, 901-905.

Passino, K. M. (2005). Biomimicry for Optimization, Control, and Automation. London, U.K.: Springer-Verlag.

Phaff, H. J., M.W. Miller, and E.M. Mrak. (1978). The Life of Yeasts. Cambridge, Massachusetts: Harvard University Press.

Riechert, S. E. (1978). Games spiders play: Behavioral variability in territorial disputes. *Behavioral Ecology and Sociobiology* **3**, 135-162.

Romanos, M. A., Scorer, C. A. and Clare, J. J. (1992). Foreign gene expression in yeast: a review. *Yeast* **8**, 423-88.

Roy, I., A. Pai, A. Lali, and M.N. Gupta. (1999). Comparison of Batch, Packed BEd and Expanded Bed Purification of *A. niger* Cellulase Using Cellulose Beads. *Bioseparation* **8**, 317-326.

Selinger, D. W., Cheung, K. J., Mei, R., Johansson, E. M., Richmond, C. S., Blattner, F. R., Lockhart, D. J. and Church, G. M. (2000). RNA expression analysis using a 30 base pair resolution Escherichia coli genome array. *Nat Biotechnol* **18**, 1262-8.

Smith, C. (2005). Striving for Purity: Advances in Protein Purification. *Nature Methods* **2**, 71-77.

Sola, A., Maaheimo, H., Ylonen, K., Ferrer, P. and Szyperski, T. (2004). Amino acid biosynthesis and metabolic flux profiling of Pichia pastoris. *Eur J Biochem* **271**, 2462-70.

Sreekrishna, K., Brankamp, R. G., Kropp, K. E., Blankenship, D. T., Tsay, J. T., Smith, P. L., Wierschke, J. D., Subramaniam, A. and Birkenberger, L. A. (1997). Strategies for optimal synthesis and secretion of heterologous proteins in the methylotrophic yeast Pichia pastoris. *Gene* **190**, 55-62.

Sun, Y., Peng, X., Zhang, Y., Lv, S. and Wang, S. (2006). Expression, purification, and characterization of human intestinal trefoil factor in Pichia pastoris. *Protein Expr Purif.*

Termonia, Y. (1994). *Macromolecules* **27**.

Teule, F. (2003). Genetic Engineering of Designed Fiber Proteins to Study Structure/Function Relationships in Fibrous Proteins. In *Department of Genetics and Biochemistry*, pp. 259. Clemson Clemson University.

Tschopp, J. F., Brust, P. F., Cregg, J. M., Stillman, C. A. and Gingeras, T. R. (1987). Expression of the lacZ gene from two methanol-regulated promoters in Pichia pastoris. *Nucleic Acids Res* **15**, 3859-76.

Villatee, F., A.S. Hussein, T.T. Bachmann. (2001). Expression Level of Heterologous Proteins in *Pichia pastoris* is Influenced by Flask Design. *Appl Microbiol Biotechnol* **55**, 463-465.

Viney, C. (1992). The Nature and Role of Liquid Crystalline Order in Silk Secretions. In *Structure, Cellular Synthesis, and Assembly of Biopolymers*, (ed. S. C. Case), pp. 256-278. New York: Springer-Verlag.

Vollrath, F. (1992). Spider Webs and Silk. *Sci. Am.* **266**, 70-76.

Vollrath, F. and Knight, D. P. (2001). Liquid crystalline spinning of spider silk. *Nature* **410**, 541-8.

Xu, M., and Lewis, R.V. (1990). Structure of a protein superfiber: spider dragline silk. *Proc. Natl. Acad. Sci. USA* **87**, 7120-7124

Yang, Y., Chen, X., Shao, Z., Zhou, P., Porter, D., Knight, D., Vollrath, F. (2005). Toughness of spider silk at high and low temperatures. *Adv. Mater.* **17**, 84-88.